Diagnosis of Cardiovascular Diseases via System Identification of Tube-Load Model

by

Shiva Ebrahimi Nejad

A thesis submitted in partial fulfillment of the requirements for the degree of

Master of Science

Department of Mechanical Engineering
University of Alberta

Abstract

Cardiovascular diseases, affecting the heart and the arteries are the leading cause of morbidity and mortality in the world. Many forms of these diseases begin and develop asymptomatically. Cardiovascular patients often not aware of the condition until later stages when the treatments are more invasive and costly. To overcome this problem, many medical researchers suggest using an active screening process for the primary diagnosis of cardiovascular diseases. This is specifically intended for patients with higher cardiovascular risk factors. However, this would not be possible without having an effective diagnostic method.

This study focuses on the diseases affecting the arteries, specifically peripheral artery disease (peripheral atherosclerosis) and arterial stiffening (arteriosclerosis). The current primary diagnosis method for these diseases includes a risk assessment, the ankle brachial index, and the flow mediated dilatation test. Although the existing methods have many advantages, they are also known to have limitations.

In order to overcome the drawbacks of these methods, this research pursued a novel method of diagnosis by applying wave analysis. This method is based on a mathematical model of the arterial tree, referred to as “tube-load model”, which simulates the arterial tree using a few easy to understand parameters, each representing a different characteristic of the arterial system.

The aforementioned diseases affect the properties of the cardiovascular system in a specific way, such as narrowing the luminal area or stiffening of compliant arteries. Since the parameters of the tube-load model reflect the characteristics of the arterial tree, analysing its parameters is a potential method to detect diseases in the arterial system.

In order to develop the diagnosis approach, the effects of the arterial diseases and arterial stiffening on the arterial tree were studied, first. Secondly, by considering the definition of each of the parameters of the tube-load model, the behavior of the tube-load parameters under these conditions were determined.

In order to validate the method, different cases of peripheral artery disease and arterial stiffening were simulated using a high-fidelity model of the arterial tree. Pressure waveforms were then used to evaluate the parameters of the tube-load model. By comparing the parameters of diseased versus normal arterial tree simulations, the proposed diagnosis method was validated.

In the next step, the sensitivity of the parameters of the tube-load model to the geometry of peripheral artery blockages were investigated. Moreover the parameter of tube-load model were used to determine the increase in the peripheral resistance. Based on the results, the tube-load model is reliable and is a promising field for future study.

Acknowledgements

First, I must thank my supervisors, Drs. Jason Carey, Jin-Oh Hahn and Sean McMurtry who guided me and supported me throughout this work. Without their help this work would have never been possible.

I would like to extend my appreciation to Dr. Olufsen who kindly provided us with her model, which was greatly helpful during my work.

I would like to extend my gratitude to my family and friends. My dear parents who always supported me during hardship and provided me with all of the help within their power. My dear friend, Elham who was more like a family member to me.

I would also like to thank my lab-mates, who made the unique and welcoming environment of our lab.

Table of Contents

List of Tables

List of Figures

1. Introduction

1.1- Motivation

Cardiovascular Disease (CVD) includes a wide range of diseases affecting the heart, blood vessels and brain vascular system. According to the World Health Organization (WHO), CVD is the leading cause of mortality and morbidity in the world [1]. From 2000 to 2010, 31% of the deaths in the United States was caused by CVD. Moreover, the total indirect and direct cost of these diseases in 2010 was approximated to be 315.4 billion of dollars [2].

CVDs may begin at very early ages and develop asymptomatically for a long time. Therefore a large portion of patients with CVD are undiagnosed. The diseases mostly stay undiagnosed until the later stages, when patients are symptomatic and the only remaining options for treatments are highly costly and invasive surgeries. However, by early detection of CVD many complications and deaths can be prevented, making most of these invasive surgeries unnecessary. Since the CVD are mostly asymptomatic, early detection is not possible without having an active monitoring system for people of higher risk of CVD, with effective diagnostic methods [1], [3]–[5].

Currently available diagnostic methods of CVD include*: i) cardiovascular risk assessment* that determines the possibility of having a CVD condition based on the general status of the patient such as the age, sex, smoking habits, etc. [6], *ii) blood pressure measurements* and its comparison with the typical value, *ii) Ankle-Brachial-Index (ABI)* which suggests using the ratio of systolic pressure at the ankle to the one of brachial artery for diagnosis of arterial disease [7], [8], *iii) Flow-Mediated-Dilation (FMD) test* that requires an ultrasound Doppler probe for measuring the change in the diameter of the artery during the heart beat in order to determine the health state of the arteries [9] or more advanced ones which are usually used for more accurate observation of the condition before surgeries, including: *iv) angiography* that involves inserting a dye into the arteries which is visible to x-rays, and *v) the Doppler ultra-sound method* which is usually used for partial monitoring of the arteries.

Wave propagation and reflection are fundamental phenomena within the arterial tree which bring

light into many characteristics of the arterial system [10], [11]. Analyzing the blood pressure waveforms may be helpful in determining the functionality of the arterial system. Tube-load model is a model of the arterial tree which accounts for the wave transmission phenomena in the arterial system, enabling such an analysis of the arterial system. In this project, the possibility of using the tube-load model for diagnosis of the cardiovascular diseases is examined.

1.2- Thesis objectivities

In this thesis a new method for diagnosis of arterial disease, based on the "tube-load model", a model of the arterial system, is proposed. The model uses a few parameters with physiological meaning to describe the wave propagation phenomena in the arteries. The diagnosis method will be finally presented as a diagnosis chart that can be used for detecting arterial diseases.

1.3- Scope of the thesis

Cardiovascular disease involves a wide range of disease, affecting the heart or the arteries. The focus of this thesis is on the diseases influencing the arterial walls, specifically: peripheral artery disease (PAD) and arterial stiffening. Moreover, while PAD mostly occurs in lower extremities, it may also affect upper extremities. Since the procedure of diagnosis is the same for the both sites, in this thesis PAD indicate diseases influencing the lower peripheral arteries. Another assumption of this project is that the patients do regular blood pressure checkups which provides a tracking system. Moreover, there are different cases of the arterial diseases, however in the validation section, the most common scenarios of these diseases are simulated and presented.

1.4- Thesis outline

This thesis is organized into 5 chapters. In Chapter 2, cardiovascular system, the diseases affecting the cardiovascular system and the diagnostics method for those diseases are covered. Chapter 3 provides a review on modeling the cardiovascular systems, including: introducing different models, the advantages and disadvantages of each model which then will be used for justifying choosing the tube-load model for diagnosis purposes. Chapter 4 presents the steps and the logic used for the proposed diagnosis method. First, the effects of the arterial diseases on the cardiovascular system will be determined using the background provided in Chapter 2, after that

the influence of the condition on the parameter of the tube-load model will be evaluated using the definition of those parameters as the basis for detecting arterial diseases. Finally the method will be validated by simulating the diseases on a high-fidelity model of the arterial tree.

In chapter 5, the sensitivity of the tube-load model to the peripheral artery disease will be studied and examined.

In chapter 6 a summary of the results of the project and future works for enhancing the method and extending the application for other cardiovascular diseases will be provided.

The mathematical basis of the tube-load model is provided in Appendix-A. The detailed information of the high-fidelity model of the arterial tree is presented in Appendix-B, as well as the full report of the simulations.

1.5- References

[1] S. Mendis, P. Puska, and B. Norrving, "Global atlas on cardiovascular disease prevention and control," *World Heal. Organ.*, pp. 2–14, 2011.

[2] A. S. Go, D. Mozaffarian, V. L. Roger, E. J. Benjamin, J. D. Berry, M. J. Blaha, S. Dai, E. S. Ford, C. S. Fox, S. Franco, H. J. Fullerton, C. Gillespie, S. M. Hailpern, J. a. Heit, V. J. Howard, M. D. Huffman, S. E. Judd, B. M. Kissela, S. J. Kittner, D. T. Lackland, J. H. Lichtman, L. D. Lisabeth, R. H. Mackey, D. J. Magid, G. M. Marcus, a. Marelli, D. B. Matchar, D. K. McGuire, E. R. Mohler, C. S. Moy, M. E. Mussolino, R. W. Neumar, G. Nichol, D. K. Pandey, N. P. Paynter, M. J. Reeves, P. D. Sorlie, J. Stein, a. Towfighi, T. N. Turan, S. S. Virani, N. D. Wong, D. Woo, and M. B. Turner, "Executive Summary: Heart Disease and Stroke Statistics--2014 Update: A Report From the American Heart Association," *Circulation*, vol. 129, no. 3, pp. 399–410, 2014.

[3] W. S. Weintraub, S. R. Daniels, L. E. Burke, B. a. Franklin, D. C. Goff, L. L. Hayman, D. Lloyd-Jones, D. K. Pandey, E. J. Sanchez, A. P. Schram, and L. P. Whitsel, "Value of primordial and primary prevention for cardiovascular disease: A policy statement from the American Heart Association," *Circulation*, vol. 124, no. 8, pp. 967–990, 2011.

[4] S. M. Grundy, T. Bazzarre, J. Cleeman, R. B. D'Agostino, M. Hill, N. Houston-Miller, W. B. Kannel, R. Krauss, H. M. Krumholz, R. M. Lauer, I. S. Ockene, R. C. Pasternak, T. Pearson, P. M. Ridker, and D. Wood, "Prevention Conference V: Beyond secondary prevention: identifying the high-risk patient for primary prevention: medical office assessment: Writing Group I.," *Circulation*, vol. 101, no. 1, pp. E3–E11, 2000.

[5] F. G. Fowkes, E. Housley, E. H. Cawood, C. C. Macintyre, C. V Ruckley, and R. J. Prescott, "Edinburgh Artery Study: prevalence of asymptomatic and symptomatic peripheral arterial disease in the general population.," *Int. J. Epidemiol.*, vol. 20, no. 2, pp. 384–392, 1991.

[6] R. B. D'Agostino, R. S. Vasan, M. J. Pencina, P. a. Wolf, M. Cobain, J. M. Massaro, and W. B. Kannel, "General cardiovascular risk profile for use in primary care: The Framingham heart study," *Circulation*, vol. 117, no. 6, pp. 743–753, 2008.

[7] G. Lawson, "The importance of obtaining ankle-brachial indexes in older adults: The other vital sign," *J. Vasc. Nurs.*, vol. 23, no. 2, pp. 46–51, 2005.

[8] L. Norgren, W. R. Hiatt, J. a. Dormandy, M. R. Nehler, K. a. Harris, F. G. R. Fowkes, and R. B. Rutherford, "Inter-Society Consensus for the management of peripheral arterial disease (TASC II)," *Int. Angiol.*, vol. 26, no. 2, pp. 82–157, 2007.

[9] M. Charakida, S. Masi, T. F. Lüscher, J. J. P. Kastelein, and J. E. Deanfield, "Assessment of atherosclerosis: The role of flow-mediated dilatation," *Eur. Heart J.*, vol. 31, no. 23, pp. 2854–2861, 2010.

[10] F. N. van de Vosse and N. Stergiopulos, "Pulse Wave Propagation in the Arterial Tree," *Annu. Rev. Fluid Mech.*, vol. 43, no. 1, pp. 467–499, 2011.

[11] N. Westerhof, P. Sipkema, G. C. Van Den Bos, and G. Elzinga, "Forward and backward waves in the arterial system," *Cardiovasc. Res.*, vol. 6, no. 6, pp. 648–656, 1972.

2. Background: Cardiovascular Diseases

This chapter includes a detailed review of the cardiovascular system, some typical diseases compromising this system such as arterial hardening and atherosclerosis, and finally, current diagnosis methods for these diseases. These diseases are also analysed in terms of their effects on the mechanical properties of the arteries. The result are used for two purposes: 1) for developing a diagnosis method based on the tube-load model; and 2) for simulating the diseases in the arterial tree simulator (Chapter 4).

2.1- Introduction

Cardiovascular Disease (CVD) (which includes the diseases affecting the heart and the arterial vessels) is the leading cause of death in the world. Early detection of CVD is an essential key toward treatment of these diseases. However, CVDs mostly develop asymptomatically. Therefore, having an effective diagnosis method is a major priority [1]. The first step to develop an effective diagnosis method is to understand the diseases, specifically: how they affect the arteries as well as blood pressure and flow waveforms. In this chapter, cardiovascular system and CVDs, specifically arterial stiffening and peripheral artery disease are studied in terms of their effects on the function of the cardiovascular system.

2.2- Cardiovascular system

2.2.1 Introduction

The blood circulation system, including the heart and blood vessels, is one of the most vital systems of the body. The main responsibility of this system is spreading the fresh blood containing vital food and gases needed by the cells all over the body and carrying back the blood again to the heart. The blood circulation system consists of two connected circulations: 1) systemic circulation and 2) pulmonary circulation.

In the systemic circulation, the fresh blood carrying all the essential particles such as oxygen and nutrients, is spread into the body in a rather complicated arterial branching system. First, the blood is pumped to the aorta which is connected to the larger arteries. The larger arteries are branched

into the smaller arteries, which are finally connected to the arterioles and capillaries reaching every single cell of the body. After the blood approaches the arterial bed, the capillaries connect to form the venules, which then join to form veins, returning the deoxygenated blood back to the right ventricle heart. In the systemic circulation, the radius of arteries decreases in bifurcations, while the total area of the two daughter arteries is bigger than the mother artery [2], [3].

The pulmonary circulation involves pumping the blood from the right ventricle into the lungs (where the product gases in the blood such as carbon dioxide are replaced by oxygen) and sending it back to the left ventricle (Figure 2–1). This study concerns the diseases associated with the systemic circulation [4].

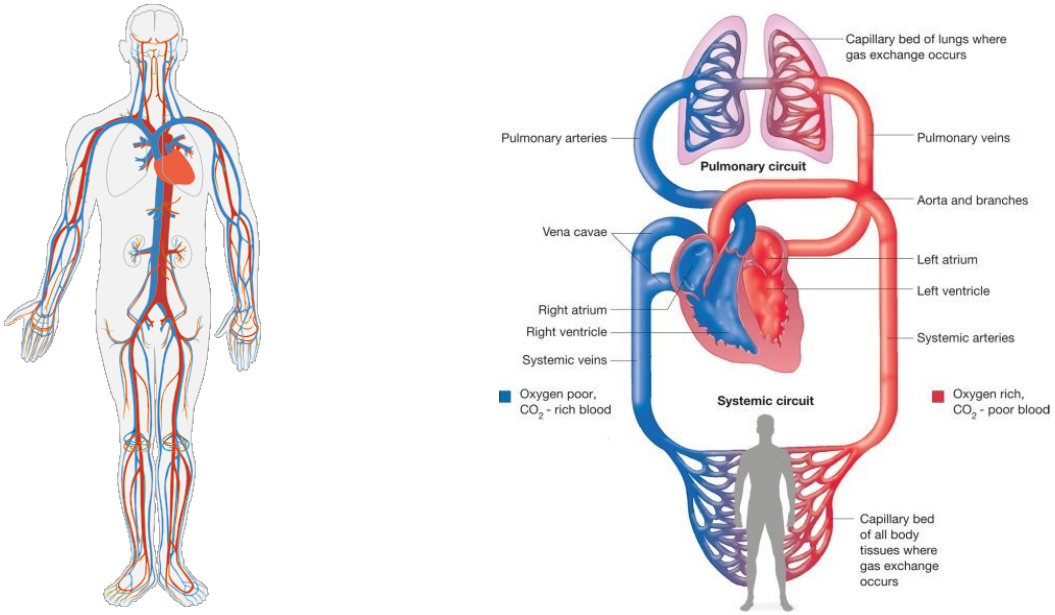

(a) **(b)**

Figure 2–1- The circulatory system: (a) Systemic circulation [4], (b) Pulmonary and systemic circulations (adapted from [49]).

2.2.2 Anatomy of the Arteries

Blood vessels have the different length, radius and structures. However, they generally consist of three main sections: the wall, the muscle and elastin section, and finally the endothelium (Figure 2–2) [3]. The heart ejects blood with an abrupt increase in blood pressure, the elastin in the arteries helps the vessels to extend as the blood pressure rises, resulting in the smooth change

in the pressure, this phenomena is referred as the cushioning function of the artery. This characteristic is modeled as the arterial compliance, which is mathematically defined as in the equation(2-1) [3], [5], [6].

$$C = \frac{\Delta V}{\Delta P} \tag{2-1}$$

with ΔV showing the change in volume in the response of ΔP change of pressure in an artery. Larger arteries such as the aorta and the iliac and the femoral arteries are consisted of more elastin than muscle, whereas for smaller vessels for instance arterioles muscle portion is more than the elastin. This difference makes larger arteries more flexible than the smaller ones. The compliance of the arterial tree is mostly provided by the large vessels [5], [7].

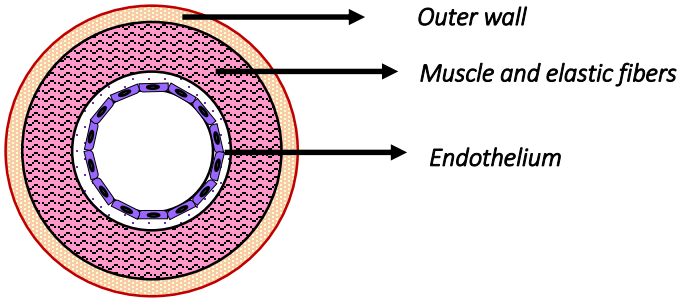

Figure 2–2 - Cross sectional view of an arterial wall [3].

2.2.3 Wave Propagation and Reflection in the Arterial Tree

One of the most important phenomena in the arterial tree is the wave propagation. The heart as a pump, sends out pressure pulse in each beat which then travels along the arteries until it reaches the arterial bed, at which point it reflects back toward the heart as shown in the Figure 2–3-(a) [8]. Therefore, as depicted in Figure 2–3-(b), the blood pressure at each point of the arterial tree is basically the summation of these forward and backward pressure waves [9]–[11]. The total pressure wave at each point is found as below:

$$P(x,t) = P_f(x,t) + P_b(x,t) \tag{2-2}$$

where P_f and P_b are forward and backward blood pressure waves, respectively. Propagation of pressure and flow waves are highly affected by the characteristics of the arterial system [10], [12],

[13]. Therefore, analysing the wave propagation in the system can give one insights about the system. Some of the parameters used for analysing the wave propagation includes: the pulse-transit-time (PTT) and the pulse-wave-velocity (PWV).

PTT is the time that takes for a pulse to transfer from the proximal point to the distal point of the same branch, traditionally measured by foot-to-foot measurement of two pulse pressure waves as shown in the Figure 2–4 [12], [14], [15]. The PWV is the mean velocity of the wave propagating in the arterial tree. PTT and PWV are related as follows:

$$PTT = \frac{d}{PWV} \tag{2-3}$$

when d is the distance between two proximal and distal point.

2.3- Cardiovascular Diseases

According to the WHO, common types of cardiovascular diseases may be categorized based on the site as shown in the Table 2-1 [1]. Among these diseases, ischemic heart disease, rheumatic heart disease, congenital heart disease, cardiomyopathies and cardiac arrhythmias affect the heart muscle and structure, whereas cerebrovascular diseases influence the blood supply to the brain [1].

In this study the main focus is on the diseases affecting arteries and arterial walls. The focus of this chapter is on arterial stiffening and peripheral arterial disease (PAD). In the following sections, a more detailed review of these two diseases will be presented.

Table 2-1 Common types of cardiovascular diseases [1], [16]**.**

Cardiovascular Disease	Definition
Ischemic Heart Disease	Disease of blood arteries supplying the heart
Cerebrovascular Disease	Disease of blood arteries supplying the brain
Aorta and Arteries Disease	Including hypertension and peripheral arteries disease
Rheumatic Heart Disease	Damage to the heart muscle and valves from rheumatic fever
Congenital heart disease	Abnormalities in heart structure present at birth
Cardiomyopathies	Disorder of the heart muscle
Cardiac arrhythmias.	Disorder of the electrical conduction system of the heart

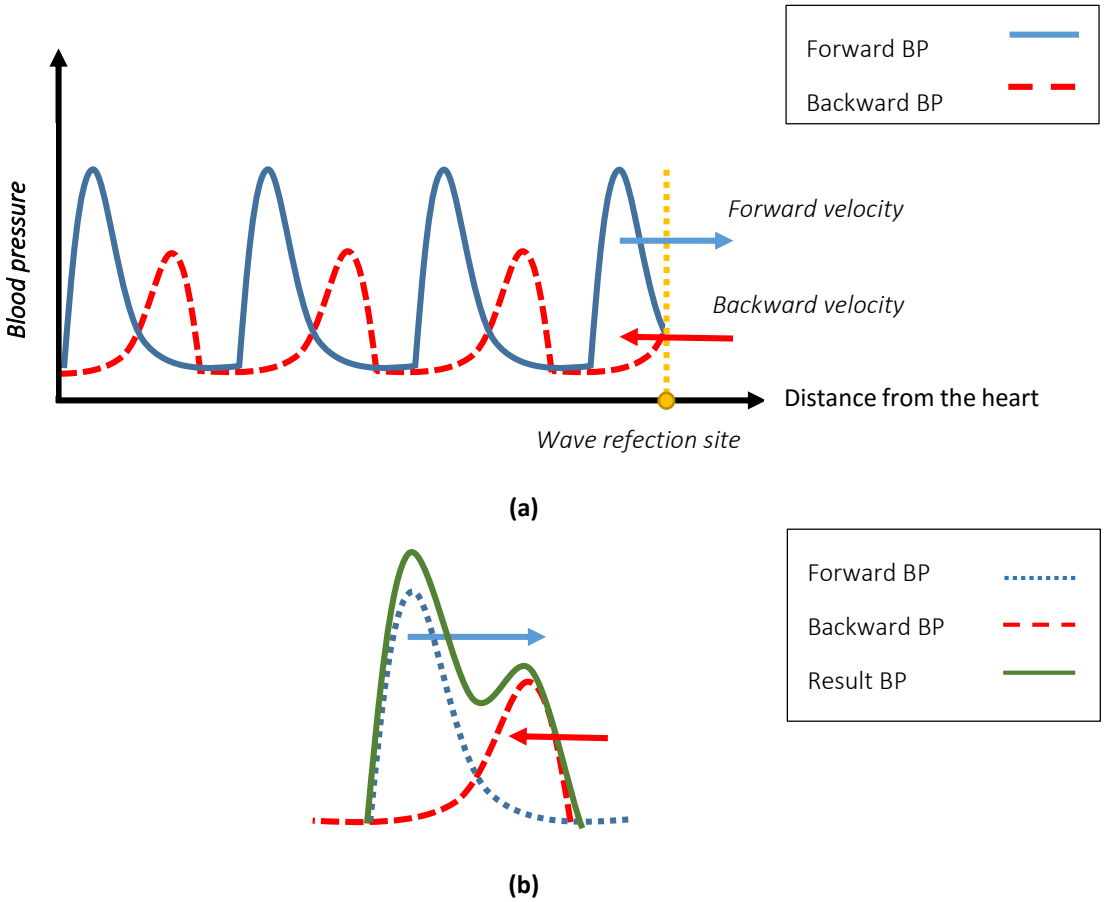

Figure 2–3 - Wave propagation phenomena in the arterial tree: (a) reflection of forward blood pressure waveform and formation of backward waveform, (b) integration of forward and backward blood pressure waveforms.

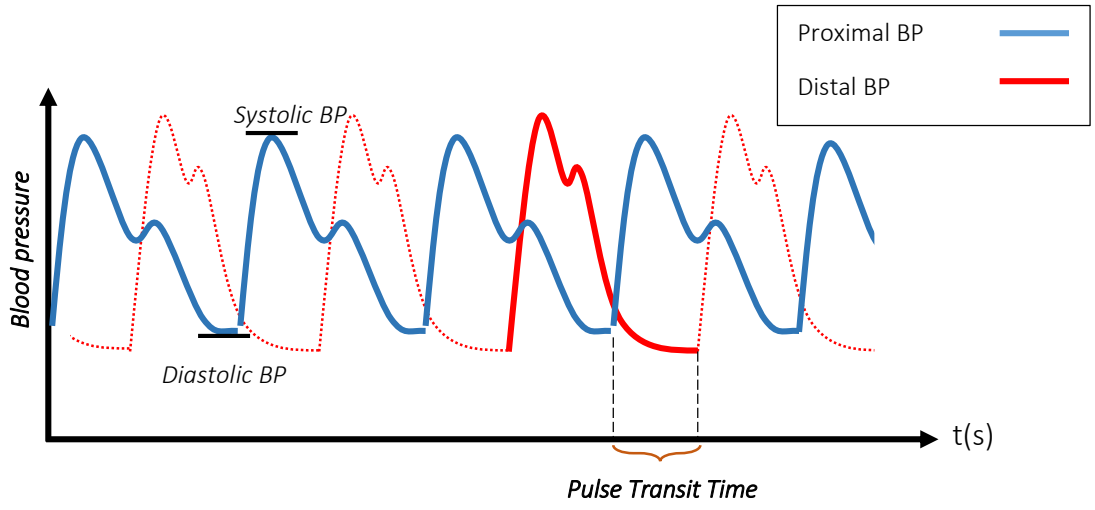

Figure 2–4 - Foot-to-foot measurement of femoral-aorta PTT.

2.3.1 Peripheral Artery Disease (PAD)

PAD are highly prevalent atherosclerosis plaques. Atherosclerosis is an inflammatory chronic autoimmune arterial disease, characterized by the deposit of fat, cholesterol or calcium plaques on the interior of the arterial walls. Plaque formation may begin just after the birth and asymptomatically develop during the patient's life. As the plaque grows, it narrows down the artery and may slow down or even block the blood flow which affects the tissues supplied by that artery (Figure 2–5). Atherosclerosis mostly occurs in large and medium-sized arteries. When these blockages form at extremities, usually legs, it is referred as peripheral artery disease or PAD [1], [17].

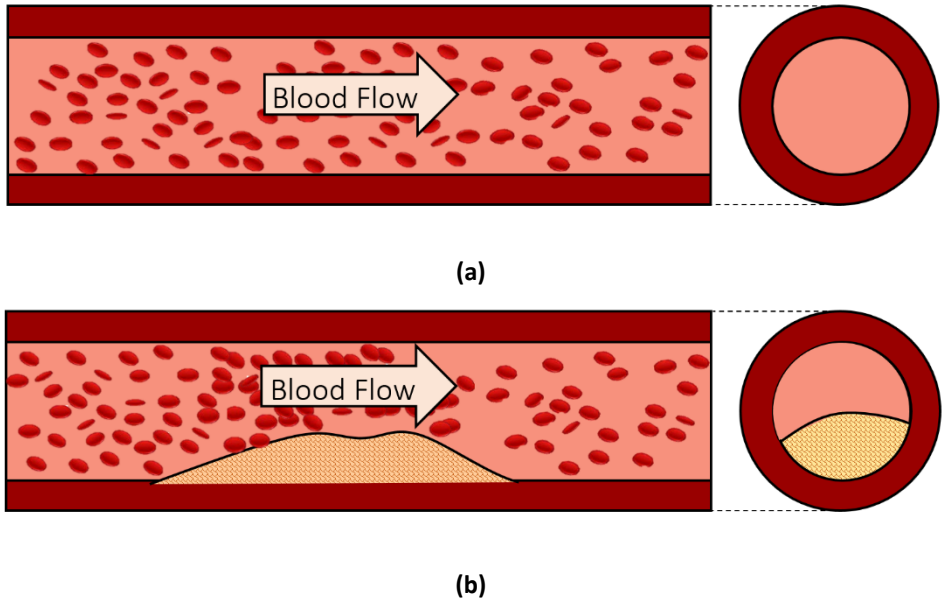

Figure 2–5 – Formation of atherosclerosis plaque: (a) cross-section of a normal artery, (b) cross-section of an artery with atherosclerosis plaque.

Symptomatic PADs usually causes pain, fatigue, pain specially during exercises (claudication) that in very advanced stages may even result in amputation of the limb [18]–[20]. PAD may not be life-threatening, but many studies have shown the existence of PAD is highly probably a manifestation of systemic atherosclerosis, which is the underlying reason for most of the CVDs [1], [17], [19], [21].

The severity of PAD may be defined based on the number of plaques, plaque sites, the length and the radius. The length of atherosclerosis lesions in the femoral artery can be up to 20cm, whereas

the luminal narrowing of cross-sectional blockage >75% is considered to be the last stage of the development of the blockage [19], [22]–[24]. PADs mostly stay asymptomatic for a long time: based on the several studies the number of asymptomatic to symptomatic PAD patients is estimated to be in the range of 1:3 to 1:4 [19], [20]. This makes the diagnosis of PAD more challenging. In fact, PADs are usually underdiagnosed in primary care practices [17], [20].

The most widely accepted method for diagnosis of PAD is ABI. This index is defined as the ratio of systolic blood pressure at the ankle to that at the brachial artery. The measurement is usually performed by a trained medical staff [19], [25].

As shown in the equations (2-4) and (2-5), ABI is measured at both right and left legs [19].

$$\text{Right ABI} = \frac{Systolic\ pressure\ at\ right\ ankle}{Systolic\ pressure\ at\ arm(right\ or\ left)} \tag{2-4}$$

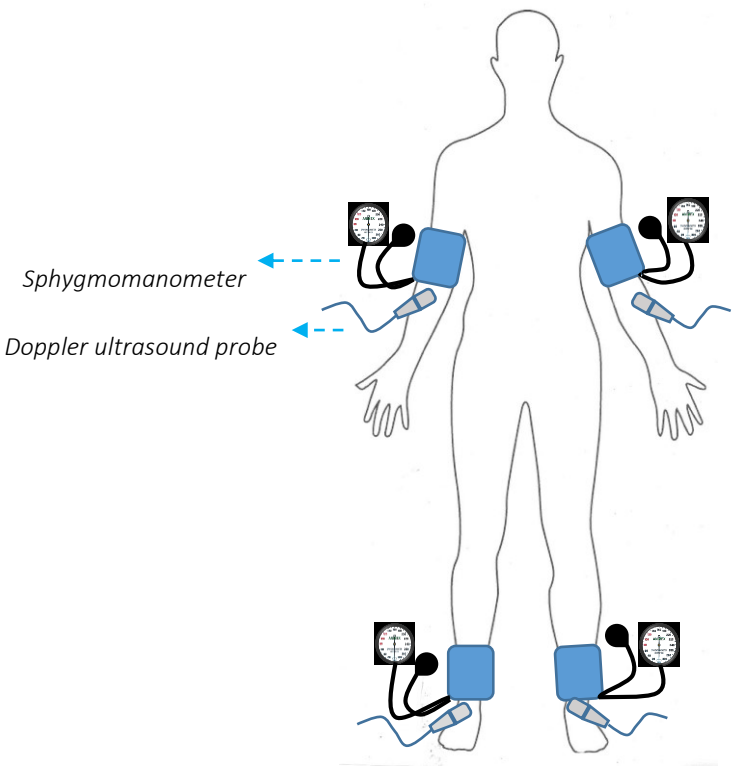

Figure 2–6 - Measuring Ankle-Brachial Index (ABI) using sphygmomanometer and Doppler ultrasound probe (adapted from [19]).

$$\text{Left ABI} = \frac{Left\ ankle\ pressure}{higher\ arm\ pressure(right\ or\ left)} \tag{2-5}$$

To measure the blood pressures at the ankle and brachial, the patient needs to be in supine position and rest for almost 15 minutes. A sphygmomanometer is used to measure the blood pressure and a Doppler ultrasound probe is also needed to detect the systolic pressure as shown in Figure 2–6. If this ratio is equal or smaller than 0.9, it might be a symptom of existence of plaques in the lower extremities[19], [26]–[28].

ABI has been proven to be an efficient diagnostic method for most of the patients with a single CVD condition that can confirm the PAD in symptomatic patients and diagnose severe PAD in patients without claudication [19]. However, ABI may give false detection in patients with multiple diseases such as patients with diabetes, vascular classification or arterial stiffening [19], [26], [29].

Another diagnosis method for diagnosing different types of CVD including PAD, is the risk assessment. This method evaluates the risk of having a CVD condition based on factors such as: gender, ethnicity, smoking, cholesterol level and diabetes, which based on the many pilot studies appear to be related to the existence of CVD [19], [25], [30]–[32]. However, the method is a population-based approach that may not be accurate for each individual. Further, in most cases additional investigation is required.

A still other diagnostic method is the flow-mediated-dilatation (FMD) test. This method is based on researches suggesting that atherosclerosis affects the endothelial vascular function of the arteries. In this test, using an ultrasound probe, the radius of the artery is measured during the systole and diastole to determine the endothelial function of the arteries.

Besides the fact that this method is usually used for systemic atherosclerosis, not the PAD, there are many other conditions affecting the endothelium, such as tobacco consumption or the phase of the cycle for the women. For the best result of the test, patients are usually asked to do pre-test preparations such as fasting and avoiding smoking. A trained medical staff as well as expensive probes and devices are required to perform this test, which makes this method challenging [33]–[35].

There are also other methods that are usually used for confirmation of primary tests and determining the location and severity of PAD mostly for pre-surgery investigation. One of these methods is Doppler ultrasound which shows the blood flow in different arteries using the ultrasound probes [36]. However, some studies have suggested false velocity determination in some cases [37].

Similar to Doppler ultrasound, magnetic resonance angiography is used for further investigation of PAD. Angiography is done by injecting a chemical liquid that makes the blood visible to the probe. Afterwards, the patient is imaged with magnetic-resonance-imaging (MRI) systems [38], [39]. Besides the expensive cost associated with this procedure, it requires dye injection which might be invasive for patients. Nevertheless, angiography and Duplex ultrasound methods show promising results on locating the PADs and determining the stage of the disease. The methods are summarized in the Table (2-2).

Table 2-2- Current method for diagnosis atherosclerosis.

Method	Application	Expenses	Requirements
ABI	Primary diagnosis of PAD	Easily affordable	Measurement systolic blood pressure: sphygmomanometer and preferably Doppler ultra-sound probe [19], [27]
Risk assessment	Primary diagnosis of CVD	Easily affordable	Assessing general risk factors: patient's information and common laboratory tests [32]
FMD	Primary diagnosis of atherosclerosis	Affordable	Measurement of the radius of the brachial artery in systolic and diastolic: ultra-sound probe [35]
Doppler Ultrasound	Further investigation of a known atherosclerotic plaques	Relatively expensive	Determining the velocity of blood flow: ultrasound probes
Angiography	Further investigation of a known atherosclerotic plaques.	Relatively expensive	Observation through the arteries: MRI system, dye injection

2.3.2 Arterial Stiffening

Arterial stiffening defines the condition of reduced flexibility of an artery to expand under the blood pressure change. Many researches have suggested that the reason underlying hypertension i.e., having a steadily higher than normal systolic and pulse pressure, is arterial stiffening [40], [41]. It is estimated that in 2011-2012, 29% of the adult population aged 18 and above in the US were suffering from hypertension, in which 83% were aware of the situation [42]. Hypertension is known to be an important risk factor of many CVDs and the root cause of many CVDs including left ventricular failure, aneurysm and even atherosclerosis [1], [40], [41], [43], [44].

Naturally, as the body gets older, the elastin in the arterial wall decreases and at the same time the wall thickens, resulting in less compliant arteries [5], [40]. Moreover, deposits of calcium in the arterial wall and accumulation of glycation end-products may also cause arterial stiffening [41]. Since the larger arteries including the aorta and carotid arteries, contain more elastin, they are more affected by the arterial stiffening, whereas femoral, iliac, brachial and radial arteries do not [5], [40].

Studying arterial stiffening is important for two reasons. First, the arterial stiffening itself is an important risk factor that is needed to be diagnosed and controlled. Second, the presence of arterial stiffening may affect the symptoms of other diseases and the diagnosis methods. Current methods for diagnosis of hypertension are listed below.

One of the none-invasive methods for determining the stiffness of conduit arteries is the measurement of PTT (or alternatively PWV). Studies have shown that as the arteries gets stiffer, the wave propagates faster, thereby increasing PWV and decreasing PTT as indicated by the equation (2-3) [13], [41], [43].

Therefore, by measuring the PWV or PTT and comparing their values with the “normal range”, one may estimate the relative stiffness of the arteries [13], [45], [46]. Evaluation the value of the PWV and PTT is done either by using the blood pressure at two superficial points or by taking advantages of the pulse wave analysis [15], [47].

ABI can also be applied for determining arterial stiffening. ABI value of 1.2 or higher may indicate

arterial stiffening [48]. However, as was discussed before, ABI usually works for a single CVD condition.

2.3.3 Result

The above discussion on the PAD and arterial stiffening can be summarized in Table 2-3. This table shows the arteries of the cardiovascular system which are affected by PAD and arterial stiffening, as well as the value of the ABI for those diseases.

Table 2-3 – Arteries affected by PAD and arterial stiffening.

Disease	Common Affected Arteries	
Peripheral Artery Disease	Iliac, Femoral, Tibials, Brachial and Radial	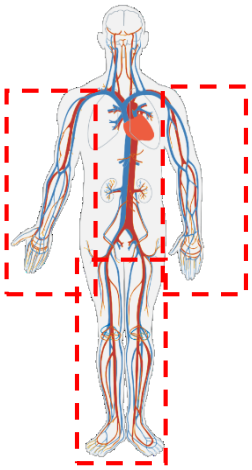 (Figure adapted from [4])
Arterial Stiffening	Aorta, Abdominal aorta and Carotids	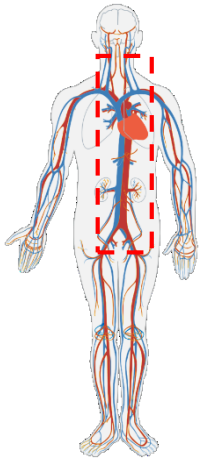 (Figure adapted from [4])

2.4- Conclusion

In this chapter, cardiovascular system, the arteries and two common types of the arterial diseases, namely PAD and arterial stiffening have been reviewed in terms of their effects on the arterial system. Furthermore, different diagnostics method of these diseases were studied.

2.5- References

[1] S. Mendis, P. Puska, and B. Norrving, "Global atlas on cardiovascular disease prevention and control," *World Heal. Organ.*, pp. 2–14, 2011.

[2] C.G. CARO, T.J. PEDLEY, R.C. SCHROTER, *The Mechanics of the Circulation*. oxford university press, 1978.

[3] C. R. Ethier and C. A. Simmons, "Introductory Biomechanics - from Cells to Organisms," *Book*, p. 545, 2007.

[4] "The circulatory ystem." [Online]. Available: https://commons.wikimedia.org/wiki/File:Circulatory_System_en.svg#/media/File:Circulatory_System_no_tags.svg.

[5] S. E. Greenwald, "Ageing of the conduit arteries," *Journal of Pathology*, vol. 211, no. 2. pp. 157–172, 2007.

[6] M. F. O'Rourke, J. a. Staessen, C. Vlachopoulos, D. Duprez, and G. E. Plante, "Clinical applications of arterial stiffness; definitions and reference values," *Am. J. Hypertens.*, vol. 15, no. 5, pp. 426–444, 2002.

[7] G. E. Mcveigh, A. J. Bank, and J. N. Cohn, "Arterial Compliance," in *Cardiovascular Medicine*, 2007, pp. 1811–1831.

[8] M. F. O'Rourke and T. Yaginuma, "Wave reflections and the arterial pulse.," *Arch. Intern. Med.*, vol. 144, no. 2, pp. 366–371, 1984.

[9] N. Westerhof, P. Sipkema, G. C. Van Den Bos, and G. Elzinga, "Forward and backward waves in the arterial system," *Cardiovasc. Res.*, vol. 6, no. 6, pp. 648–656, 1972.

[10] G. Swamy, N. B. Olivier, and R. Mukkamala, "Calculation of forward and backward arterial waves by analysis of two pressure waveforms," *IEEE Trans. Biomed. Eng.*, vol. 57, no. 12, pp. 2833–2839, 2010.

[11] G. Zhang, J. O. Hahn, and R. Mukkamala, "Tube-load model parameter estimation for

monitoring arterial hemodynamics," *Front. Physiol.*, vol. 2 NOV, no. November, pp. 1–18, 2011.

[12] F. N. van de Vosse and N. Stergiopulos, "Pulse Wave Propagation in the Arterial Tree," *Annu. Rev. Fluid Mech.*, vol. 43, no. 1, pp. 467–499, 2011.

[13] G. F. Mitchell, H. Parise, E. J. Benjamin, M. G. Larson, M. J. Keyes, J. a. Vita, R. S. Vasan, and D. Levy, "Changes in arterial stiffness and wave reflection with advancing age in healthy men and women: The Framingham Heart Study," *Hypertension*, vol. 43, no. 6, pp. 1239–1245, 2004.

[14] J. C. Bramwell and a. V. Hill, "The Velocity of the Pulse Wave in Man," *Proc. R. Soc. B Biol. Sci.*, vol. 93, no. 652, pp. 298–306, 1922.

[15] J. Solà, O. Chételat, C. Sartori, Y. Allemann, and S. F. Rimoldi, "Chest pulse-wave velocity: A novel approach to assess arterial stiffness," *IEEE Trans. Biomed. Eng.*, vol. 58, no. 1, pp. 215–223, 2011.

[16] World Health Organization, "Cardiovascular diseases (CVDs) Fact Sheet No. 317," *World Health Organization Media center*, 2015. [Online]. Available: http://www.who.int/mediacentre/factsheets/fs317/en/.

[17] A. T. Hirsch, "Peripheral Arterial Disease Detection, Awareness, and Treatment in Primary Care," *JAMA J. Am. Med. Assoc.*, vol. 286, no. 11, pp. 1317–1324, 2001.

[18] D. S. G. Conway, J. Heeringa, D. a M. Van Der Kuip, B. S. P. Chin, A. Hofman, J. C. M. Witteman, and G. Y. H. Lip, "The Rotterdam Study," 2003.

[19] L. Norgren, W. R. Hiatt, J. a. Dormandy, M. R. Nehler, K. a. Harris, F. G. R. Fowkes, and R. B. Rutherford, "Inter-Society Consensus for the management of peripheral arterial disease (TASC II)," *Int. Angiol.*, vol. 26, no. 2, pp. 82–157, 2007.

[20] "About Peripheral Artery Disease (PAD)," *American Heart Association*. [Online]. Available: http://www.heart.org/HEARTORG/Conditions/More/PeripheralArteryDisease/About-Peripheral-Artery-Disease-PAD_UCM_301301_Article.jsp.

[21] A T. Hirsch, S. L. Halverson, D. Treat-Jacobson, P. S. Hotvedt, M. M. Lunzer, S. Krook, S. Rajala, and D. B. Hunninghake, "The Minnesota Regional Peripheral Arterial Disease Screening Program: toward a definition of community standards of care.," *Vasc. Med.*, vol. 6, no. 2, pp. 87–96, 2001.

[22] G. Pasterkamp, P. J. Wensing, M. J. Post, B. Hillen, W. P. Mali, and C. Borst, "Paradoxical arterial wall shrinkage may contribute to luminal narrowing of human atherosclerotic femoral arteries.," *Circulation*, vol. 91, no. 5, pp. 1444–1449, 1995.

[23] S. Dalager, E. Falk, I. B. Kristensen, and W. P. Paaske, "Plaque in superficial femoral arteries indicates generalized atherosclerosis and vulnerability to coronary death: An autopsy study," *J. Vasc. Surg.*, vol. 47, no. 2, pp. 296–302, 2008.

[24] A. Farb, A. L. Tang, A. P. Burke, L. Sessums, Y. Liang, and R. Virmani, "Sudden coronary death. Frequency of active coronary lesions, inactive coronary lesions, and myocardial infarction.," *Circulation*, vol. 92, no. 7, pp. 1701–1709, 1995.

[25] H. J. Willens, W. Davis, D. M. Herrington, K. Wade, K. Kesler, S. Mallon, W. V. Brown, J. H. C. Reiber, and J. K. Raines, "Relationship of Peripheral Arterial Compliance and Standard Cardiovascular Risk Factors," *Vasc. Endovascular Surg.*, vol. 37, no. 3, pp. 197–206, 2003.

[26] S. a Carter, "Indirect systolic pressures and pulse waves in arterial occlusive diseases of the lower extremities.," *Circulation*, vol. 37, no. 4, pp. 624–637, 1968.

[27] G. Lawson, "The importance of obtaining ankle-brachial indexes in older adults: The other vital sign," *J. Vasc. Nurs.*, vol. 23, no. 2, pp. 46–51, 2005.

[28] T. J. Orchard and D. E. Strandness, "Assessment of peripheral vascular disease in diabetes: report and recommendation of an international workshop," *Diabetes Care*, vol. 83, no. 12, pp. 685–695, 1993.

[29] S. C. Nam, S. H. Han, S. H. Lim, Y. S. Hong, J. H. Won, J. I. Bae, and J. Jo, "Factors affecting the validity of ankle-brachial index in the diagnosis of peripheral arterial obstructive disease.," *Angiology*, vol. 61, no. 4, pp. 392–396, 2010.

[30] S. M. Grundy, T. Bazzarre, J. Cleeman, R. B. D'Agostino, M. Hill, N. Houston-Miller, W. B. Kannel, R. Krauss, H. M. Krumholz, R. M. Lauer, I. S. Ockene, R. C. Pasternak, T. Pearson, P. M. Ridker, and D. Wood, "Prevention Conference V: Beyond secondary prevention: identifying the high-risk patient for primary prevention: medical office assessment: Writing Group I.," *Circulation*, vol. 101, no. 1, pp. E3–E11, 2000.

[31] M. Naghavi, E. Falk, H. S. Hecht, M. J. Jamieson, S. Kaul, D. Berman, Z. Fayad, M. J. Budoff, J. Rumberger, T. Z. Naqvi, L. J. Shaw, O. Faergeman, J. Cohn, R. Bahr, W. Koenig, J. Demirovic, D. Arking, V. L. M. Herrera, J. Badimon, J. a. Goldstein, Y. Rudy, J. Airaksinen, R. S. Schwartz, W. a. Riley, R. a. Mendes, P. Douglas, and P. K. Shah, "From Vulnerable Plaque to Vulnerable Patient-Part III: Executive Summary of the Screening for Heart Attack Prevention and Education (SHAPE) Task Force Report," *Am. J. Cardiol.*, vol. 98, no. 2 SUPPL. 1, pp. 2–15, 2006.

[32] R. B. D'Agostino, R. S. Vasan, M. J. Pencina, P. a. Wolf, M. Cobain, J. M. Massaro, and W. B. Kannel, "General cardiovascular risk profile for use in primary care: The Framingham heart study," *Circulation*, vol. 117, no. 6, pp. 743–753, 2008.

[33] A. J. Flammer, T. Anderson, D. S. Celermajer, M. a. Creager, J. Deanfield, P. Ganz, N. M. Hamburg, T. F. Lüscher, M. Shechter, S. Taddei, J. a. Vita, and A. Lerman, "The assessment of endothelial function: From research into clinical practice," *Circulation*, vol. 126, no. 6, pp. 753–767, 2012.

[34] M. Stout and S. Aims, "Integration of Flow Mediated Dilatation Into Clinical Practise ."

[35] M. Charakida, S. Masi, T. F. Lüscher, J. J. P. Kastelein, and J. E. Deanfield, "Assessment of atherosclerosis: The role of flow-mediated dilatation," *Eur. Heart J.*, vol. 31, no. 23, pp. 2854–2861, 2010.

[36] "Duplex ultrasound." [Online]. Available: https://www.nlm.nih.gov/medlineplus/ency/article/003433.htm.

[37] A. T. Hirsch, Z. J. Haskal, N. R. Hertzer, C. W. Bakal, M. A. Creager, J. L. Halperin, L. F. Hiratzka, W. R. C. Murphy, J. W. Olin, J. B. Puschett, K. A. Rosenfield, D. Sacks, J. C. Stanley, L. M. Taylor, C. J. White, J. White, R. A. White, E. M. Antman, S. C. Smith, C. D. Adams, J. L. Anderson, D. P. Faxon, V. Fuster, R. J. Gibbons, J. L. Halperin, L. F. Hiratzka, S. A. Hunt, A. K. Jacobs, R. Nishimura, J. P. Ornato, R. L. Page, and B. Riegel, "ACC/AHA 2005 Practice Guidelines for the Management of Patients With Peripheral Arterial Disease (Lower Extremity, Renal, Mesenteric, and Abdominal Aortic)," *Circulation*, vol. 113, no. 11, pp. e463–e465, 2006.

[38] H. M. Bonel, B. Saar, H. Hoppe, H. H. Keo, M. Husmann, K. Nikolaou, K. Ludwig, Z. Szucs-Farkas, S. Srivastav, and R. Kickuth, "MR angiography of infrapopliteal arteries in patients with peripheral arterial occlusive disease by using Gadofosveset at 3.0 T: diagnostic accuracy compared with selective DSA.," *Radiology*, vol. 253, no. 3, pp. 879–890, 2009.

[39] D. C. Goff, D. M. Lloyd-Jones, G. Bennett, S. Coady, R. B. D'Agostino, R. Gibbons, P. Greenland, D. T. Lackland, D. Levy, C. J. O'Donnell, J. G. Robinson, J. S. Schwartz, S. T. Shero, S. C. Smith, P. Sorlie, N. J. Stone, and P. W. F. Wilson, "2013 ACC/AHA guideline on the assessment of cardiovascular risk: A report of the American college of cardiology/American heart association task force on practice guidelines," *Circulation*, vol. 129, no. 25 SUPPL. 1, 2014.

[40] Z. Sun, "Aging, Arterial Stiffness, and Hypertension," *Hypertension*, vol. 65, no. 2, pp. 252–256, 2014.

[41] H.-Y. Lee and B.-H. Oh, "Aging and arterial stiffness.," *Circ. J.*, vol. 74, no. 11, pp. 2257–2262, 2010.

[42] T. Nwankwo, S. S. Yoon, V. Burt, and Q. Gu, "Hypertension among adults in the United States: National Health and Nutrition Examination Survey, 2011-2012.," *NCHS Data Brief*, no. 133, pp. 1–8, 2013.

[43] M. AlGhatrif, J. B. Strait, C. H. Morrell, M. Canepa, J. Wright, P. Elango, A. Scuteri, S. S. Najjar, L. Ferrucci, and E. G. Lakatta, "Longitudinal trajectories of arterial stiffness and the role of blood pressure: The Baltimore longitudinal study of aging," *Hypertension*, vol. 62, no. 5, pp. 934–941, 2013.

[44] A. V. Chobanian, G. L. Bakris, H. R. Black, W. C. Cushman, L. a. Green, J. L. Izzo, D. W. Jones, B. J. Materson, S. Oparil, J. T. Wright, and E. J. Roccella, "Seventh report of the Joint National Committee on Prevention, Detection, Evaluation, and Treatment of High Blood Pressure," *Hypertension*, vol. 42, no. 6, pp. 1206–1252, 2003.

[45] R. Kelly, C. Hayward, a Avolio, and M. O'Rourke, "Noninvasive determination of age-related changes in the human arterial pulse.," *Circulation*, vol. 80, no. 6, pp. 1652–1659, 1989.

[46] O. Vardoulis, T. G. Papaioannou, and N. Stergiopulos, "On the Estimation of Total Arterial Compliance from Aortic Pulse Wave Velocity," *Ann. Biomed. Eng.*, vol. 40, no. 12, pp. 1–8, 2012.

[47] X. F. Teng and Y. T. Zhang, "An evaluation of a PTT-based method for noninvasive and cuffless estimation of arterial blood pressure," *Annu. Int. Conf. IEEE Eng. Med. Biol. - Proc.*, pp. 6049–6052, 2006.

[48] S. Hyun, N. I. Forbang, M. a. Allison, J. O. Denenberg, M. H. Criqui, and J. H. Ix, "Ankle-brachial index, toe-brachial index, and cardiovascular mortality in persons with and without diabetes mellitus," *J. Vasc. Surg.*, vol. 60, no. 2, pp. 390–395, 2014.

[49] "Blood circulation." [Online]. Available: http://clogged-arteries.howthingis.com/heart-disease-articles/.

3. Background: Modeling the Cardiovascular System

In this chapter, different types of mathematical models of cardiovascular system are reviewed. These models include lumped models, distributed-parameter models, 3-dimensional models and tube-load models. The models are compared in terms of accuracy, complexity and their potential application in the diagnosis of cardiovascular diseases. This chapter provides the basis for developing and validating a diagnostic method of cardiovascular diseases in Chapter 4.

3.1- Introduction

The cardiovascular system is one of the fundamental systems of the body. This system includes the heart pumping the blood and the blood vessels transporting the blood to and from the heart. There have been many efforts and experiments trying to mathematically model this complicated system, resulting in the development of different models from different perspectives with various applications.

These arterial models can be divided into four main categories: lumped models, distributed models, three-dimensional models and tube-load models. The most well-known type of the lumped models is the Windkessel model, which was proposed by Frank in 1899 [1]. In Windkessel model the arterial tree is modeled with a few electrical elements, such as resistance and capacitance, representing the peripheral resistance and the total arterial compliance, respectively. The main advantage of the Windkessel models is its simplicity. However, Windkessel model does not take into account the wave reflection and propagation in the arterial tree and is thus usually used to determine the flow at the aorta based on the corresponding pressure or visa-versa [2]–[4].

A more accurate type of model is the distributed parameter models. These models break down the entire arterial tree into smaller segments and then solve the one-dimensional Navier-Stokes equations for each segment. Distributed models account for the wave propagation, branching, geometrical and mechanical properties of different sections of the arterial system, and therefore, provide one of the most accurate models of this system [5]–[8]. However, these models require much information about the system, including the mechanical properties and geometry.

Moreover, the boundary conditions are also hard to determine [9].

Three-dimensional (3D) models provide a 3D description of the flow waveform using the computational fluid dynamics (CFD) theories. Similar to the distributed parameter models, these models also require the knowledge of geometry and mechanical properties of the system. Due to the high burden of the calculations in these models, their application is limited to a small section of the arterial system, such as a part of the carotid, or a bifurcation site [10], [11]. As in the distributed models, 3D models also require a large amount of information about the properties of the system.

Finally, tube-load models describe the arterial system with a tube connected to a load. The tube represents the main artery of the system, namely the aorta, whereas the load represents the peripheral resistance and compliance [12]–[15]. Unlike the Windkessel models, the tube models account for wave propagation and reflection phenomena in the arterial tree. In comparison with the distributed parameter model, the tube-load model is less complicated with fewer parameters. Furthermore, the parameters of the tube-load model have the physiological meaning which may give insights into the physiologic states of the arterial tree.

The final goal of this chapter is to determine if any of these models are applicable for diagnostic purposes. Such a model has to provide an accurate analysis of the pressure and flow waveforms. To this end, in this chapter the introduced models are reviewed in terms of the accuracy, applications, requirements, complexity and the potentials to be used as a diagnostic tool.

3.2- Models of the Arterial Tree

The arterial models can be categorized into four main types: lumped models, parametric models, 3-dimensional models and tube-load models. In this section, these models are examined and discussed.

3.2.1 Lumped Models

Lumped models are simplified models of an arterial system, simulating the whole system with a few parameters. One of the most well-known lumped models is the Windkessel model, proposed by Frank in 1899 [1]. The simplest possible of this kind is the two-element Windkessel model, which

has a resistance and a compliance, representing the total peripheral resistance and arterial compliance of the arterial tree.

Therefore, this model accounts for the ability of the artery to store blood and the resistance of the peripheries against the blood flow [1], [2]. Figure 3–1(a) shows a schematic of an artery while Figure 3–1(b) depicts the Windkessel model of the same artery.

Windkessel models provide a general description of the relation between the pressure and the flow in the proximal aorta with a few parameters [1], [18]. In order to improve the model, another elemnt representing the characteristic impedance of the artery was added as the third parameter of the Windkessel model, as shown in the Figure 3–2(a) [17]. The four-element model has an additional resistance as depicted in Figure 3-2(b), which was shown to be more accurate in reproducing the pressure waveforms [3].

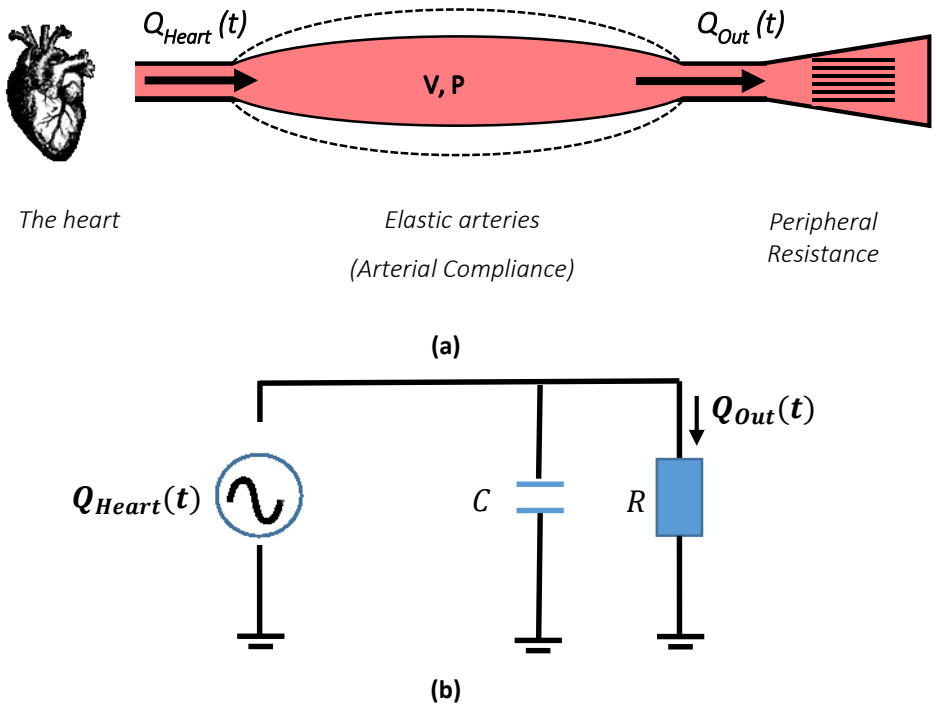

Figure 3–1 – A compliant artery (a): The two-element Windkessel model of the artery (adapted from [4]), (b): Equivalent electrical circuit based on the Windkessel model (adapted from [16]).

Nevertheless, the Windkessel models consider infinite wave propagation velocity for the arterial tree and, therefore, do not account for the wave reflection and propagation in the arterial tree, which makes these models less ideal in reproducing blood pressure and flow waveforms.

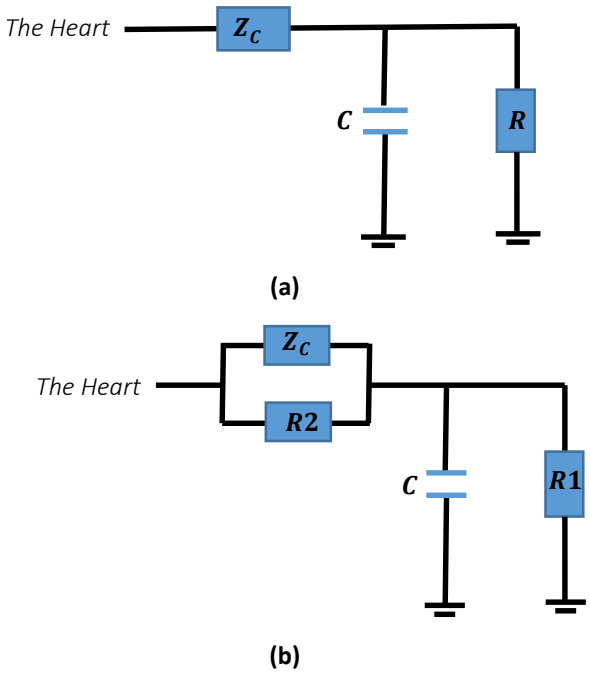

Figure 3–2 – Different types of the Windkessel model (a) Three-element (adapted from [17]) and (b) four-element Windkessel models (adapted from [3]).

3.2.2 Distributed Parameter Models

In distributed parameter models, the whole arterial tree is divided into smaller segments for which the information about the geometry and the mechanical properties are required. The flow waveforms are then analyzed either by the Womersley's theory of "oscillatory flow in the arteries" or the 1-dimensional Navier-Stokes equations for conservation of mass and momentum in flow waveforms [19], [9].

These models usually account for the tapering of the arteries along their lengths, multiple branching and variable mechanical properties of the arterial system. Some of these models are discussed as follows.

One of the early works of this model was the analysis of the pressure and flow propagation in the human leg, in which the one-dimensional flow problem in an elastic tube was solved using the finite difference method, for geometrically and mechanically defined branched tubes [20]. A more complicated model was the development of the model of the total arterial system, which considers the whole system as 128 small uniform elastic segments for studying the effect of special conditions in the arterial system [6]. One of the other models of the total arterial system simulated

the arterial tree as 28 smaller segments connected to each other with the tapering of the arteries along their length also being considered and the peripheries being simulated as a structured tree. The result was then validated by the experimental measurement of the flow data [5], [21].

Distributed parameter models give an accurate estimation of the flow and the pressure that can predict the waveforms at any desired site of the arterial system. However, there are a lot of information about the properties of the system that are required to be determined [22]. Information on the geometry itself requires a magnetic resonance imaging (MRI) or Doppler ultrasound investigation, whereas direct measurement of the mechanical properties such as the elastic properties.

3.2.3 Three Dimensional Models

Another method for simulating the behavior of the flow and pressure waveforms in the blood vessel is the three-dimensional (3-D) models, which provide a detailed analysis of the hemodynamics. Similar to the distributed parameter method, this model also requires information regarding the geometry and mechanical properties of the part of the system which is under study [9]. Moreover, the 3D models usually involve very complicated simulations. Therefore, they are usually used for analyzing a specific part of the cardiovascular system and under a pathological condition such as: atherosclerosis and aneurysm [23] due to the heavy burden associated with the calculation.

A more complicated model of this type is a coupled model, joining a partial 3D model of the flow dynamics using the Navier-Stokes equation with the lumped model of the arterial system in order to make the model more coherent with the rest of the arterial tree and more accurate [24].

3D models provide a very detailed and accurate analysis of the hemodynamics. However, they require prior measurement of the system characteristics such as the geometrical and mechanical properties.

3.2.4 Tube Models

The other type of the arterial tree models is the so-called “tube-load” model. This type of models takes advantages of the analogy between the voltage wave propagation in the transmission line

and the pressure waveform propagation in the arterial tree. By applying this analogy, tube-load model simulates the large arteries such as the aorta as a tube with the characteristic impedance of Z_C, representing the wave propagation path, while simulating the peripheral load as a load with its impedance of Z_L (Figure 3–3) [12].

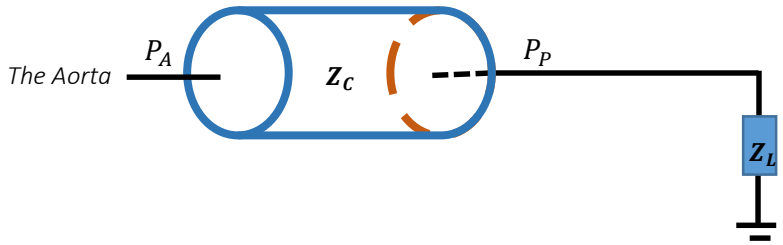

Figure 3–3- Tube-load model.

The load is usually a combination of the different electrical elements such as the resistance (R_T) and the capacitance (C_T) and the characteristic impedance of the conduit artery. The resistance represents the peripheral resistance and the capacitance stands for the peripheral compliance of the system. The peripheral load shows the reflection site at which the flow waveform transferring into the peripheries reflects back toward the heart, as depicted in Figure 3-4. Another parameter of the tube-load model is the pulse-transit-time, which is the transfer time of the pulse to get from one (proximal) end of the tube to the other (distal) end.

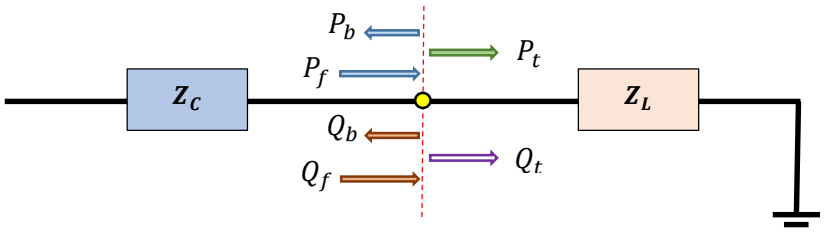

Figure 3–4 - Wave reflection at the peripheries.

Even though the tube-load model is a simple model with only a few parameters, it accounts for the wave propagation and the wave reflection phenomena in the arterial tree.

The aortic blood pressure and flow, provide much information regarding the condition and the well-being of cardiovascular system while the measurement around the aortic valve are highly invasive. The tube-load model is its potential application in determining the aortic blood pressure

or alternatively flow, by using the peripheral blood pressure [13], [25].

3.3- Discussion

In this chapter, a review of different models of the arterial system was presented and summarized in Table 3-1. These models are usually used for two purposes; first, for forward modeling, which uses the characteristics of the system to evaluate the output of the system based on the physics theories, and second, the inverse modeling, which uses the input and output of the system to determine the model. Inverse modeling is useful in monitoring the arterial tree.

The final goal of this chapter was to select a model that is potentially applicable for the diagnosis purposes. One such model should be accurate in analyzing the waveforms and preferably be suitable for parameter identification.

The study shows that the lumped models, such as the Windkessel models provide a simple mathematical model of the arterial tree with a few parameters which is suitable for parameter identification. However, Windkessel models overlook the wave propagation and reflection phenomena in the arterial tree and consequently are less accurate. Moreover, Windkessel models are usually used to derive a mathematical relation between flow and the pressure at the aorta, while measuring the flow and the pressure in the aorta are highly invasive. Therefore, the Windkessel models are not a convenient model for diagnostic purposes.

Distributed parameter models and 3D models provide a patient-specific analysis of this system which is the most accurate methods available. While the 3D models can only be applied to a local area of the arterial system, 1D models actually can simulate the whole arterial system. However, these models require determining a large number of parameters of the system characteristics in order to estimate the waveform information at different sites in the arterial tree. From the parameter identification perspective, however, this type of model needs the determination of excessively many parameters that is virtually impossible.

Tube-load models consider the wave reflection and propagation phenomena in the arterial tree, which make them more accurate than the Windkessel model. In contrast to the distributed parameter models, they are parsimonious and have less parameters. Therefore, the tube-load

Table 3-1 - Models of the arterial tree.

Models	Advantages	Disadvantages
Lumped model	• Simplicity • Physiological meaning	• Assuming an infinite speed of waves • Not accurate
Distributed parameter models	• Accuracy	• Require prior investigation of the characteristics of the arterial system
3D models	• Accuracy	• Require prior investigation of the characteristics of the arterial system • Complexity • Local application
Tube-load models	• Simplicity • Relatively accurate • Considering the wave propagation phenomena • Physiological meaning	• Only analyses the two ends of the tube

models seem to have a desirable balance between the accuracy and simplicity while considering the wave transmission. These models are also convenient for parameter identification purposes. In fact, the parameters of the tube-load model can be determined if there is access to 2 waveforms of the arterial system [13], [26].

Moreover, the parameters of tube-load models have physiological meaning. Therefore, the tube-load model brings light to many characteristics of the arterial system that might be useful in detecting diseases in the arterial system. In the next chapter, the possibility of using the tube-load model for diagnostic applications is discussed. The mathematical background is also presented in Appendix-A.

3.4- Conclusion

In this chapter, different mathematical models of the arterial tree were reviewed. The potential applications of the tube-load models over other models for diagnostic purposes, was justified. In the next chapter, the diagnosis method using tube-load model will be developed and discussed.

3.5- References

[1] K. Sagawa, R. K. Lie, and J. Schaefer, "Translation of Otto Frank's Paper 'Die Grundform des Arteriellen Pulses' Zeitschrift fur Biologie 37: 483-526 (1899)," *J. Mol. Cell. Cardiol.*, vol. 22, no. 3, pp. 253–277, 1990.

[2] Y. Shim, A. Pasipoularides, C. a. Straley, T. G. Hampton, P. F. Soto, C. H. Owen, J. W. Davis, and D. D. Glower, "Arterial windkessel parameter estimation: A new time-domain method," *Ann. Biomed. Eng.*, vol. 22, no. 1, pp. 66–77, 1994.

[3] N. Stergiopulos, B. E. Westerhof, and N. Westerhof, "Total arterial inertance as the fourth element of the windkessel model.," *Am. J. Physiol.*, vol. 276, no. 1 Pt 2, pp. H81–H88, 1999.

[4] N. Westerhof, J. W. Lankhaar, and B. E. Westerhof, "The arterial windkessel," *Med. Biol. Eng. Comput.*, vol. 47, no. 2, pp. 131–141, 2009.

[5] M. S. Olufsen, C. S. Peskin, W. Y. Kim, E. M. Pedersen, A. Nadim, and J. Larsen, "Numerical simulation and experimental validation of blood flow in arteries with structured-tree outflow conditions," *Ann. Biomed. Eng.*, vol. 28, no. 11, pp. 1281–1299, 2000.

[6] A. Avolio, "Multi-branched model of the human arterial system," *Med. Biol. Eng. Comput.*, vol. 18, no. 6, pp. 709–718, 1980.

[7] N. Stergiopulos, D. F. Young, and T. R. Rogge, "Computer simulation of arterial flow with applications to arterial and aortic stenoses," *J. Biomech.*, vol. 25, no. 12, pp. 1477–1488, 1992.

[8] S. J. Sherwin, L. Formaggia, J. Peiro, and V. Franke, "Computational modelling of 1D blood flow with variable mechanical properties and its application to the simulation of wave propagation in the human arterial system," *Int. J. Numer. Methods Fluids*, vol. 43, no. 6–7, pp. 673–700, 2003.

[9] F. N. van de Vosse and N. Stergiopulos, "Pulse Wave Propagation in the Arterial Tree," *Annu. Rev. Fluid Mech.*, vol. 43, no. 1, pp. 467–499, 2011.

[10] J. Dong, K. K. L. Wong, and J. Tu, "Hemodynamics analysis of patient-specific carotid bifurcation: A CFD model of downstream peripheral vascular impedance," *Int. j. numer. method. biomed. eng.*, vol. 29, no. 4, pp. 476–491, 2013.

[11] S. E. Lee, S. W. Lee, P. F. Fischer, H. S. Bassiouny, and F. Loth, "Direct numerical simulation of transitional flow in a stenosed carotid bifurcation," *J. Biomech.*, vol. 41, no. 11, pp. 2551–2561, 2008.

[12] G. Zhang, J. O. Hahn, and R. Mukkamala, "Tube-load model parameter estimation for monitoring arterial hemodynamics," *Front. Physiol.*, vol. 2 NOV, no. November, pp. 1–18, 2011.

[13] M. Rashedi, N. Fazeli, a Chappell, S. Wang, R. MacArthur, M. S. McMurtry, B. a Finegan, and J. O. Hahn, "Comparative Study on Tube-Load Modeling of Arterial Hemodynamics in Humans," *ASME J. Biomech.*, vol. 135, no. March, p. 31005, 2013.

[14] L. R. John, "Forward electrical transmission line model of the human arterial system.," *Med. Biol. Eng. Comput.*, vol. 42, no. 3, pp. 312–321, 2004.

[15] N. Westerhof, P. Sipkema, G. C. Van Den Bos, and G. Elzinga, "Forward and backward waves in the arterial system," *Cardiovasc. Res.*, vol. 6, no. 6, pp. 648–656, 1972.

[16] C. R. Ethier and C. A. Simmons, "Introductory Biomechanics - from Cells to Organisms," *Book*, p. 545, 2007.

[17] N. Westerhof, G. Elzinga, and P. Sipkema, "An artificial arterial system for pumping hearts.," *J. Appl. Physiol.*, vol. 31, no. 5, pp. 776–781, 1971.

[18] N. Stergiopulos, J. J. Meister, and N. Westerhof, "Evaluation of methods for estimation of total arterial compliance.," *Am. J. Physiol.*, vol. 268, no. 4 Pt 2, pp. H1540–H1548, 1995.

[19] J. R. Womersley, "Oscillatory flow in arteries: the constrained elastic tube as a model of arterial flow and pulse transmission.," *Phys. Med. Biol.*, vol. 2, no. 2, pp. 178–187, 1957.

[20] J. K. Raines, M. Y. Jaffrin, and A. H. Shapiro, "A computer simulation of arterial dynamics in the human leg.," J. Biomech., vol. 7, no. 1, pp. 77–91, 1974.

[21] M. S. Olufsen, "Structured tree outflow condition for blood flow in larger systemic arteries.," *Am. J. Physiol.*, vol. 276, no. 1 Pt 2, pp. H257–H268, 1999.

[22] S. L. Zhaopeng Fan, Gong Zhang, and Simon Liao, "Pulse Wave Analysis, Advanced Biomedical Engineering", Dr. Gaetano Gargiulo (Ed.), 2011. Available from: http://www.intechopen.com/books/advanced-biomedical-engineering/pulse-wave-analysis

[23] C. a Taylor and C. a Figueroa, "Patient-specific modeling of cardiovascular mechanics.," *Annu. Rev. Biomed. Eng.*, vol. 11, pp. 109–134, 2009.

[24] A. Quarteroni and A. Veneziani, "Analysis of a geometrical multiscale model based on the coupling of odes and pdes for blood flow," Multiscale Modeling & Simulation, vol. 1, no. 2, pp. 173–195, 2003.

[25] J. O. Hahn, A. T. Reisner, F. A. Jaffer, and H. H. Asada, "Subject-specific estimation of central aortic blood pressure using an individualized transfer function: A preliminary feasibility study," *IEEE Trans. Inf. Technol. Biomed.*, vol. 16, no. 2, pp. 212–220, 2012.

[26] J.O. Hahn, "A system identification approach to non-invasive central cardiovascular monitoring," Thesis (Ph. D.)--Massachusetts Institute of Technology, Dept. of Mechanical Engineering, 2008.

4. CVD Diagnosis via System Identification of Tube-Load Model

In this chapter a novel method for diagnosis of common types of arterial diseases: peripheral artery disease and arterial stiffening, is presented. This method is based on a mathematical model of the arterial tree called the "tube-load model", which was previously introduced in Chapter 3. Later in this chapter, the proposed method will be validated using an arterial tree simulator.

4.1- Introduction

Cardiovascular disease (CVD) is the number one cause of death in the world, responsible for 17.3 million deaths worldwide per year [1]. CVDs may begin and develop asymptomatically. Thus, the patients may not become aware of their CVD condition until late stages, while in many cases, sudden cardiac arrest is the first manifestation of the disease [1], [2]. From this standpoint, having an effective diagnosis method is crucial for helping the patients with CVD. In fact, many studies are suggesting active monitoring of people of higher risk of having CVD [1], [3], [4]. There are many types of CVD, affecting the heart or the arteries. The main focus of this project is on the diseases affecting the arteries.

Today's most prevalent diagnostic method for the arterial diseases is to use the direct investigation and measurements of system properties including the systolic, diastolic and mean blood pressure and then to compare those values with the range defined as the normal values [5].

Another detection method is the Ankle-Brachial-Index (ABI), defined as the ratio between the systolic blood pressure at the ankle and the one for brachial artery [5], [6]. The ABI is the most widely accepted method and easy to perform. However, the effectiveness of ABI method is under question for patient who are experiencing other diseases, such as diabetes and vascular calcification and CVD at the same time [5]–[7].

An alternative diagnostic method is the risk assessment based on the lifestyle and current health status of the patients. Some of these factors include: age, smoking habits, diabetes mellitus and obesity [4]. Another test for diagnosis of peripheral artery disease (PAD) is the flow-mediated dilatation (FMD) test, which uses the endothelial function as a marker for the diagnosis. FMD

requires using the ultrasonic probe which must be done in the medical center by professionals [8].

In this chapter, a potential method for detecting the artery diseases is presented to overcome the above mentioned drawbacks associated with currently used detection methods. The method is based on the tube-load model, which is a mathematical model of the arterial system characterized by a few parameters. The model accounts for the wave propagation and reflection phenomena in the arterial tree and therefore reveals more information about the arterial system in comparison with the direct markers and population-based method such as risk assessment and ABI.

The parameters of the tube-load model are equipped with physiological implications and indicate different characteristics of the cardiovascular system. Since the arterial diseases affect the characteristics of the system, we hypothesize that analyzing the tube-load model parameters may enable the detection of characteristic changes in the arterial system and may thus be used as the diagnostic markers.

Finally, in this project, the feasibility of using the tube-load model parameters for diagnosis of the arterial diseases will be validated using an arterial tree simulator in which different conditions of arterial diseases are simulated, for each of which, tube-load model parameters will be evaluated. The parameters will then be used for detecting the arterial diseases and the success of the model would be discussed.

4.2- Tube-Load Model

"Tube-load" model is a model for simulating the behavior of the arterial tree. This model describes the behavior of the arterial tree using few parameters, namely: characteristic impedance, peripheral resistance, peripheral compliance and pulse transit time (PTT). There are many arrangements of these parameters, the one used in this paper is shown in Figure 4–1. As it is derived in appendix-A, for a single loss-less tube-load model, the pressure waveforms at the two ends of an artery, represented as a tube, is related as described below [9], [10]:

$$\frac{P_{Aorta}}{P_P} = \frac{e^{j\omega\tau} + \Gamma . e^{-j\omega\tau}}{1 + \Gamma} \tag{4-1}$$

with P_{Aorta} and P_P being the blood pressure at any time in the aorta and the peripheries,

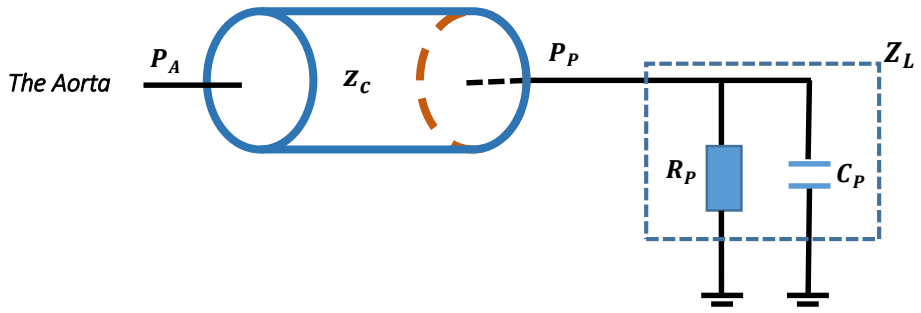

Figure 4–1- Tube-load model.

respectively. In this equation τ stands for the pulse transit time. Moreover, Γ indicates the coefficient of reflection defined as follows:

$$\Gamma = \frac{Z_L - Z_C}{Z_L + Z_C} \tag{4-2}$$

with Z_L and Z_c indicating the load and the characteristic impedances [9]. Moreover, for the tube-load model shown in the Figure 3–3, the load impedance is calculated as follows:

$$Z_L = \frac{R_P}{R_P C_P j\omega + 1} \tag{4-3}$$

Therefore, by replacing equation (4-3) into the equation (4-2), the coefficient of reflection is calculated to be:

$$\Gamma = \frac{R_P - Z_C(R_P C_P + 1)j\omega}{R_P + Z_C(R_P C_P + 1)j\omega} \tag{4-4}$$

Substituting equation (4-4) into the equation (4-1) leads to the following:

$$\frac{P_{Aorta}}{P_P} = \frac{(R_P + Z_C(R_P C_P + 1)j\omega)e^{-j\omega\tau} + (R_P - Z_C(R_P C_P + 1)j\omega).e^{j\omega\tau}}{2R_P} \tag{4-5}$$

the equation can then be simplified as shown in the equation (4-6).

$$\frac{P_{Aorta}}{P_P} = \frac{(1 + (Z_C C_P + Z_C/R_P)j\omega)e^{-j\omega\tau} + (1 - (Z_C C_P + Z_C/R_P)j\omega).e^{j\omega\tau}}{2} \tag{4-6}$$

By defining the new parameters $\alpha = Z_C C_P$ and $\beta = Z_C/R_P$., the equation (4-6) can be rewritten as follows:

$$\frac{P_{Aorta}}{P_P} = \frac{(1 + (\alpha + \beta)j\omega)e^{-j\omega\tau} + (1 - (\alpha + \beta)j\omega).e^{j\omega\tau}}{2} \quad (4\text{-}7)$$

In order to translate the equation (4-7) into the discrete time domain, the equation is first translated into the Laplace domain as shown in the equation (4-8).

$$\frac{P_{Aorta}}{P_P} = \frac{(1 + (\alpha + \beta)s)e^{-s\tau} + (1 - (\alpha + \beta)s).e^{s\tau}}{2} \quad (4\text{-}8)$$

moreover, in order to transfer the equation into the discretized space, the forward difference approximation with a sampling frequency of f_s , s is approximated to $s \approx f_s(z-1)$. Using this approximation the equation (4-8) is rewritten as follows:

$$\frac{P_{Aorta}(k)}{P_P(k)} = \frac{(1 + (\alpha + \beta)(f_s(z-1)))z^n + (1 - (\alpha + \beta)f_s(z-1))z^{-n}}{2} \quad (4\text{-}9)$$

with n=$f_s.\tau$. As this equation verifies, once the parameters α and β are known, aortic blood pressure can be derived from measured the blood pressure at peripheries such as the radial or femoral. Likewise, it can be shown that by having access to the P_{Aorta} and P_P waveform, the parameters α and β can be determined. In order to determine the tube-load model parameters with having two blood pressure waveforms at the aorta and the femoral, the equation (4-9) can be rewritten as follows:

$$\begin{aligned}\hat{P}_{Aorta}(k) = {} & \big(1 - f_s(\alpha + \beta)\big)P_P(k-n) + f_s(\alpha + \beta)P_P(k-n+1) \\ & + \big(1 + f_s(\alpha + \beta)\big)P_P(k+n) - f_s(\alpha + \beta)P_P(k+n+1)\end{aligned} \quad (4\text{-}10)$$

in this equation $\hat{P}_{Aorta}$ is the tube-load approximation of the blood pressure at the aorta.

4.2.1 Parameters of the Tube-Load Model

i. Arterial Resistance:

The Windkessel theory, models each compliant artery, as a flexible chamber that experience a time-varying pressure. For this artery, the resistance can be estimated as follows:

$$R_{art} = \frac{\bar{P}_{art}}{\bar{Q}_{art}} \tag{4-11}$$

with R_{art} indicating the resistance of the artery, $\bar{P}_{art}$ mean pressure in the artery and $\bar{Q}_{art}$ the flow in the artery [11]. Therefore, the peripheral resistance is defined before as below:

$$R_P = \frac{\bar{P}_p}{\bar{Q}_p} \tag{4-12}$$

On the other hand, for a laminar flow of a Newtonian fluid with the viscosity μ in a horizontal circular tube with the length "l"and radius "r", as shown in the Figure 4–2, the pressure drop can be predicted as shown in the equation (4-13)[12].

$$\Delta P = \frac{8\mu l Q}{\pi r^4} \tag{4-13}$$

Therefore the viscous resistance of the fluid is calculated as below:

$$R = \frac{8\mu l}{\pi r^4} \tag{4-14}$$

As the equation (4-14) suggests, the total resistance of the arterial tree is mainly due to the smaller arteries and the resistance of the larger arteries such as the aorta, can be neglected in comparison with smaller arteries.

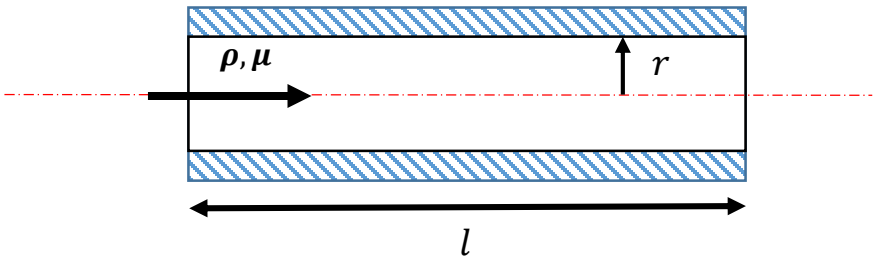

Figure 4–2 - Calculating the resistance of a tube.

ii. Arterial compliance

For the tube described in the Windkessel theory, the ratio of the change in the volume for a known change of pressure is described as the compliance, mathematically defined as in the equation (4-15).

$$C_{tube} = \frac{dv}{dP} \tag{4-15}$$

with v and P showing the volume and the pressure of the artery. Cross-sectional compliance, is the compliance of per unit length of the tube, which is defined as shown in the equation (4-16) [13].

$$C_{Cross-Sectional} = \frac{dA}{dP} \tag{4-16}$$

In which the dP and dA show the local change is the lumen area and pulse pressure respectively. Change in the lumen area is also calculated as below [13]:

$$dA = \pi.({D_s}^2 - {D_d}^2)/4 \tag{4-17}$$

With D_s and D_d indicating the systolic and diastolic diameter of that section. dA can also be approximated as follows:

$$dA = \pi.(dD).D/2 \tag{4-18}$$

In this equation, D is the average diameter and dD is the change in diameter. Therefore the cross-sectional compliance can also be defined as in the equation (4-18) [14].

$$C_{Cross-Sectional} = \frac{(dD)}{2dP}\pi D \tag{4-19}$$

On the other hand, Young's modulus of an artery, can be related to the arterial compliance as follows [14].

$$E = \frac{dP}{dD}\frac{D}{h} \tag{4-20}$$

with E showing the Young's modulus per length of wall thickness of the artery. Therefore,

$$C_{Cross-Sectional} = E\frac{\pi D^2}{2h} \tag{4-21}$$

As the peripheries can be assumed as multiple smaller tubes attached together, the total

compliance is the integration of the smaller ones. For each smaller tube, the compliance may be calculated using the equation (4-21).

However, due to the limitations in measurement in the extremities, it is not possible to find a quantitative measurement of the peripheral compliance, but it might be possible to determine its qualitative behavior.

iii. Characteristic impedance

Another parameter of the tube-load model, is characteristic impedance or Z_c of the tube which is defined as in the equation (4-22) [9].

$$Z_c = \sqrt{\frac{l_{tube}}{C_{tube}}} \tag{4-22}$$

Moreover pulse transit time (PTT) for the same tube, is estimated as follows [9].

$$PTT = L\sqrt{l_{tube}.C_{tube}} \tag{4-23}$$

In the equations (4-22) and (4-23), l_{tube} and C_{tube} indicate the inertance and compliance respectively. The inertance is defined as below:

$$l_{tube} = \int_0^L C_u \frac{\rho}{A(x)} dx \tag{4-24}$$

at which, ρ is the density of the blood, where L is the length of the segment, A is the area of the cross section which varies along the tube [15]. In order to account for the non-flat velocity profile of the blood flow, the coefficient of C_u is also added, which is approximated to be around 4/3 [15].

4.3- Diagnosis Algorithm

4.3.1 Atherosclerotic Blockage

Atherosclerosis is defined as the formation of the abnormal blockages in the arteries. These blockages mostly happen in the peripheries, which are referred to as peripheral arterial disease

(PAD). In the case of PAD, the main tube of the tube-load model is left unchanged, while the peripheries are affected by the growth of the abnormal masses in the arterial wall as shown in the Figure 4–6. The effect of the PAD on each of the parameters of the tube-load model is discussed below.

a. *Characteristic Impedance:*

As it was mentioned before, the characteristic impedance is a function of the inertance and the compliance of the main tube of the tube-load model. In this study, the main tube is the aortic-femoral tube, which is not affected by the blockages in the peripheries. Therefore, it is anticipated that in the case of the PAD, the characteristic impedance of the tube is left unchanged.

b. *Pulse Transit Time*

As it was mentioned for the characteristic impedance, since in the case of the PAD the tube inertance and compliance are not affected, based on the equation (4-23) the PTT is also expected to remain the same in the process of the formation of the stenosis.

c. *Peripheral Resistance*

The resistance of an artery can be approximated by Poiseuille law as shown in the equation (4-14). Considering this equation, as the open area of an artery reduces, the resistance on that part will increase, whereas the length of the blockage is directly proportional to the resistance. Therefore, growing in the blockages of the peripheries results in an increase in the magnitude of the peripheral resistance.

d. *Peripheral Compliance*

Formation of a blockage in an artery, results in the decrease of the lumen area, increase of stiffness and increase in the wall thickness. Therefore, based on the equation (4-37), the cross-sectional compliance of an artery will decrease as the blockage grows. Moreover the site, the radius, the length and the stiffness of the blockage affect the value of the peripheral compliance.

4.3.2 Arterial Stiffening

In case of the arterial hardening, the stiffness of the arteries increases, which then make the affected arteries less compliant. Arterial stiffening may influence any artery of the arterial system, but it mostly affects the larger arteries such as the aorta. Therefore, in most cases of arterial stiffening, the tube is subjected to change in the characteristics, whereas the peripheries are usually left unaffected [16]. The effect of this alteration in the stiffness of the tube on the tube-load model parameters is discussed below.

a. *Characteristic Impedance:*

In case of arterial stiffening, the elasticity of the arteries is compromised; the arteries affected by this situation get stiffer. As the equation (4-21) supports, arterial stiffening makes the arteries less compliant by increasing the Young's modulus. In the tube-load model, the total compliance of the tube is integration of different arteries, including the aorta, abdominal aorta, iliac and part of the femoral. Since in case of arterial stiffening, based on the equation (4-22) and (4-25) C_{tube} decreases while the inertance is constant, it can be shown that the Z_c of the tube will increase.

b. *Pulse Transit Time:*

As it was discussed for the characteristic impedance, in case of the arterial stiffening, the compliance of the tube decreases and the inertance is constant, therefore, based on the equation (4-24), it is expected that the PTT of the tube reduces as the aorta gets stiffer. In fact, there has been many experiments and researches supporting this statement [17], [18]. In fact, the relation between PTT and the compliance of the arterial tree is such that there has been researches suggesting estimating the tube compliance using the PTT or PWV [19], [20].

c. *Peripheral Resistance:*

Arterial stiffening mostly affects the larger arteries and leaves the peripheries untouched. Therefore, in case of the arterial stiffening the peripheral resistance is expected to be the same as the one of a healthy arterial tree.

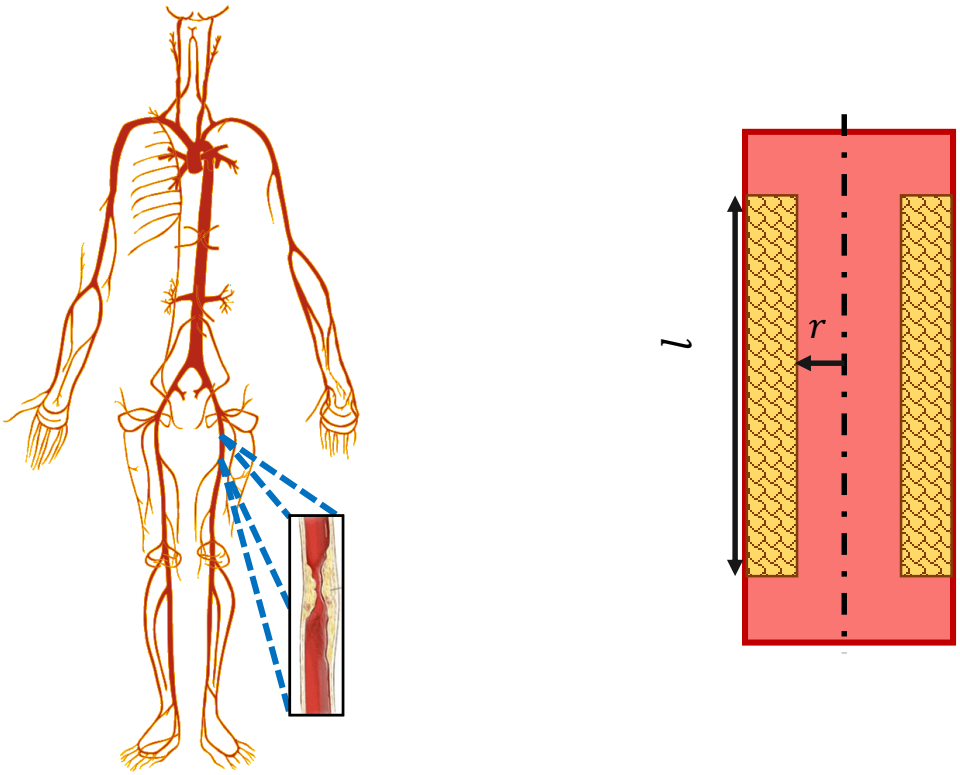

(a) (b)

Figure 4–3 - Femoral stenosis, (a) growth of femoral stenosis (adapted from [24]) and (b) simplified geometry of a femoral stenosis with length l and radius r.

d. *Peripheral Compliance:*

As it was mentioned for the peripheral resistance, since the peripheral arteries are left unchanged in case of the arterial disease, the peripheral compliance is anticipated to remain the same in case of arterial stiffening as well.

4.3.3 Effect of Arterial Diseases on Identifiable Tube-Load Model Parameters

Based on the previous discussions the effects of the arterial diseases on the tube-load model parameters can be summarized in the Table 4-1. When the blood pressure waveforms of the two ends of the tube are used as the input of tube-load model, the parameters α, β and PTT will be identified.

Therefore, in order to check the possibility of using the tube - load model as a diagnostic method, it is essential to check the effect of the arterial diseases on these parameters. Using Table 4-1, the

effects of the arterial diseases can be summarized as in the Table 4-2.

Table 4-1 - Qualitative effect of atherosclerosis and arterial stiffening on the parameters of the tube-load model.

$\boldsymbol{Parameters}$	***Arterial Stiffening***	***Atherosclerotic Blockage***
PTT	↓	Not affected
Z_c	↑	Not affected
C_p	Not affected	↓
R_p	Not affected	↑

Table 4-2 shows two main points, first the tube-load model is sensitive to both arterial stiffening and PAD cases, second the change in the parameters for these two cases of arterial diseases is in a way that the model can also differ these diseases. Therefore, if the method is verified to work as shown in the Table 4-2, it can detect arterial stiffening and PAD's.

Table 4-2 - Effect of the atherosclerosis and the arterial stiffening on the tube-load model parameters.

$\boldsymbol{Parameters}$	***Arterial Stiffening***	***Atherosclerotic Blockage***
PTT	↓	Constant
$\alpha = Z_C C_P$	↑	↓
$\beta = Z_C / R_P$	↑	↓

4.4- Methods

4.4.1 High-Fidelity Arterial Tree Simulator

In order to verify the proposed method, a high fidelity simulator of arterial tree was used [21], [22]. In this simulator the blood is considered as a non-compressible fluid, Newtonian flow that runs through viscoelastic tubes with different length and radius which taper along their length. The whole arterial tree is divided into 29 smaller tubes branching along the arterial tree, until it gets to the peripheries which are modeled as a structured tree (Figure 4-4).

The simulator is a subject-specific model, for which geometries of the each of the artery, including the length, inlet and outlet radii and the properties of the structured tree were set as they were measured for a man of age 32 using the magnetic resonance images (MRI). The radius in zero pressure of each artery is assumed to a function of x as shown below [21]:

$$r_o(x) = r_t \exp\left(\log(\frac{r_b}{r_t})\frac{x}{L}\right) \tag{4-25}$$

with x showing the distance to the top side of the associated tube, L the length of that tube, and r_t and r_b indicate the inlet and outlet radius respectively as shown in the Figure 4–5.

1- Ascending aorta
2- Anonyma
3- Subclavian And brachial
4- Right carotid
5- Aortic arc
6- Left carotid
7- Aortic arc
8- Subclavian and brachial
9- Thoracic aorta
10- Celiac axis
11- Abdominal aorta
12- Superior mesenteric
13- Abdominal aorta
14- Renal
15- Abdominal aorta
16- Renal
17- Abdominal aorta
18- Inferior mesenteric
19- Abdominal aorta
20- External iliac
21- Femoral
22- Internal iliac
23- Deep femoral
24- Femoral

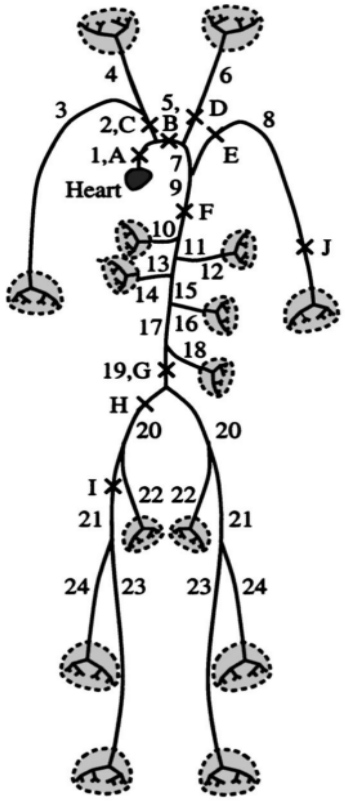

Figure 4–4 - The cardiovascular system modeled in the arterial tree simulator [21].

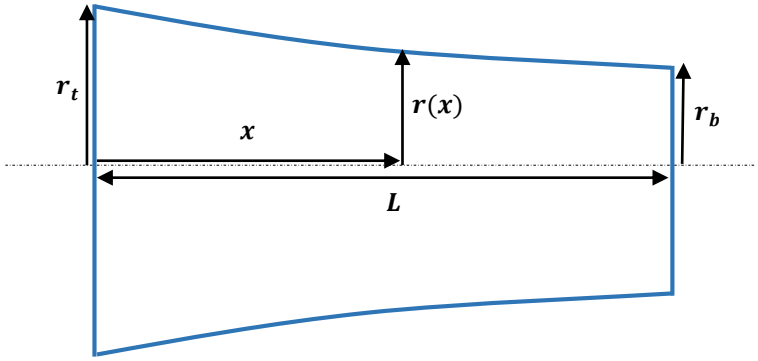

Figure 4–5 – Tapering along the length of an artery (adapted from [21]).

The flow waveforms at different sites of the body were also recorded using the MRI techniques for the same subject. This simulator then solves the 1-dimensional axisymmetric Navier-Stokes equations for the defined arterial tree by using one non-invasive flow measurement at ascending aorta and calculates the flow and pressure waveforms at different sites of the cardiovascular system including femoral, brachial and etc. Afterward the result of the simulation is compared with the actual value of flow data at the measurement sites[1] [21], [22]. In this project, this simulator was used to simulate arterial diseases; two main features of the simulator that were directly used for this project are discussed in the following sections:

i. Simulating Arterial Stiffening

There are different indices for describing the arterial stiffness including: arterial dispensability, arterial compliance, volume elastic modulus, circumferential Young's modulus and etc. [16]. In the simulator the value of parameter Eh/r_o is set in order to describe the stiffness at each tube, in which E is circumferential Young's modulus, h is the arterial wall thickness and r_o is the radius at zero pressure condition. It was shown that the value of Eh/r_o can be estimated using the following exponential function [21]:

$$\frac{Eh}{r_o} = C_1 \exp(C_2 . r_o) + C_3 \tag{4-26}$$

The value of constants in this equation, were estimated to be $C_1 = 2.00 \times 10^7\ g.s^{-2}.cm^{-1}$, $C_2 = -22.53\ cm^{-1}$ where $C_3 = 8.65 \times 10^5\ g.s^{-2}.cm^{-1}$ according to [22]. For each point of an artery the radius is calculated using equation (4-25). For simulating arterial stiffening, the value of C_1 and C_3 were multiplied to a coefficient of $K(= (\frac{Eh}{r})/\left(\frac{Eh}{r}\right)_{Normal})$ defining the severity of the disease. In this project, different scenarios of arterial hardening were simulated, among which the most common type of arterial stiffening which is when the aorta is affected as presented in Table 4-3.

In these simulations, the values of stiffness were set to increase from 20% up to 100% of the normal value [16], [23].

[1] For more detailed regarding the simulator refer to appendix-B.

ii. Simulating PAD

In case of PAD, the part of the artery, which is subjected to the disease, narrows down. However, it is not possible to locally change the cross-sectional area of an artery in this simulator. The solution adapted to address this issue was to divide the whole subjected artery into three sections as shown in the Figure 4–6, the first and the last sections would be left unchanged while the radius of the middle part will be reduced to represent the existence of the blockage.

On the other hand, in the simulator at each bifurcation, the artery should be connected to two other elements such as an artery or a structured tree. Therefore, in order to divide the artery, at each split the artery is connected to the next section of the artery and a dummy structured tree[2]. Using this method, different cases of PAD in the femoral artery with various lengths and radiuses were simulated. The length and the blockage value are set based on the experimental research on PADs [5]. In the Table 4-4 part of these simulations with 30% and 50% of blockage and different length are presented.

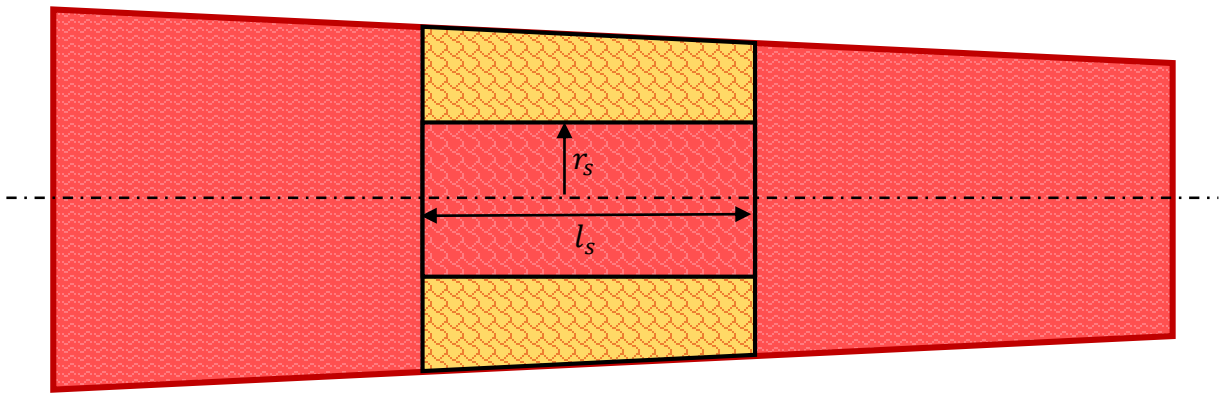

Figure 4–6 – Adding blockage into the artery: dividing the artery into three sections.

4.4.2 Tube-Load Modeling

After simulating different cases of arterial stiffening and the PAD, the next step is to determine the parameters of the tube-load model for each case and compare that with ones of the simulation of a normal arterial tree. In order to determine the parameters, two of the waveforms namely:

[2] Adding the blockage into the arteries is explain in the appendix-B.

aortic and femoral was exported from the simulations.

For all of the simulations, the aortic pressure was exported from a consistent point in the aorta which was 10 cm after the aortic valve, whereas the femoral pressure waveforms, were measured at a point in the femoral (artery 24 in the Figure 4–4) which was 12 cm after the bifurcation of femoral and deep femoral. The sampling frequency of the simulations was $F_s = 1000\ Hz$.

One of the most important applications of the tube-load model, is to determine the pressure in the aorta, based on a non-invasive measurement at the periphery. Therefore, one method to determine the functionality of the tube - load model, is to evaluate its accuracy in reproducing the aortic pressure.

Thus the error in the parameter estimation was defined as the difference between the estimated blood pressure and the actual blood pressure in the aorta. The error was defined using the root-mean-squared-error (RMSE). For the aortic pressure estimation the RMSE was defined as shown below:

$$RMSE = \sqrt{\frac{1}{n}\sum_{i=1}^{n}\left(P_{Aorta}(i) - \hat{P}_{Aorta}(i)\right)^2} \tag{4-27}$$

In this equation, $\hat{P}_{Aorta}(i)$ is the estimation of aortic blood pressure based on the tube-load model, whereas the P_{Aorta} shown the actual blood pressure in the aorta and finally n is the size of the data. Therefore the $RMSE$ can be considered as the cost function for determining the unknown parameters including α, β and PTT. The parameters were then estimated using a nonlinear multivariable function in MATLAB. After estimating the parameters, the aortic blood pressure can be reproduced by using the equation (4-10) and the estimated value of the parameters.

In order to validate the accuracy of the tube-load model for reproducing the aortic pressure, first this procedure will be applied for determining the aortic blood pressure for an actual subject. To do so the blood pressure data were recorded from a patient under open heart surgery at the University of Alberta Hospital. The data collection was made upon the approval by the University of Alberta Health Research Ethics Board (ID Pro00021889) and informed consent from the

patients. At the next step, the same procedure was done for simulations of different cases of arterial stiffening and PAD in the femoral artery.

4.5- Result

First the tube-load model was applied to the blood pressure data collected from a patient. The actual versus estimated aortic blood pressure of this patient is shown in the Figure 4–7.

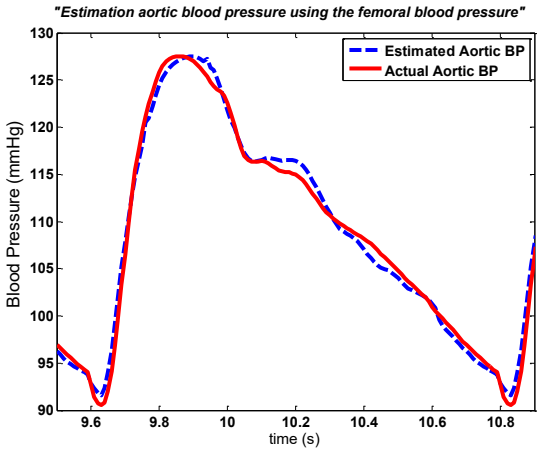

Figure 4–7 - Using tube-load model for estimating aortic BP.

After simulating different cases of diseases and exporting the data, the tube-load model parameters α, β and PTT were determined. In order to validate the ability of the tube-load model to reproduce the aortic blood pressure for these CVD simulations, the RMSE error was also calculated. The reconstructed versus the actual aortic blood pressure waveforms for one case of arterial stiffening and one case of PAD in the lower extremities are shown in the Figure 4–8(a) and Figure 4–8(b) respectively. The parameter estimation result are presented in the Table 4-3 and Table 4-4. In these tables, simulation number 0, indicate the normal arterial tree, in which no abnormal stiffening or PAD exists. For arterial stiffening cases, the aorta was subjected to stiffening, the value of stiffness (defined as $\frac{Eh}{r}$) was multiplied by the value of k from 1 to 2. The result of the simulation, including the variables α, β, PTT and $RMSE$ is also depicted in the Table 4-4. In simulations of PAD in the femoral artery, there are two parameters that can be set, the area and the length of the blockages. In this chapter, two different blockages of 30% and 50%, with length 2 to 10 cm are presented. The value of variables α, β, PTT and $RMSE$ for these simulations are depicted in Table 4-4.

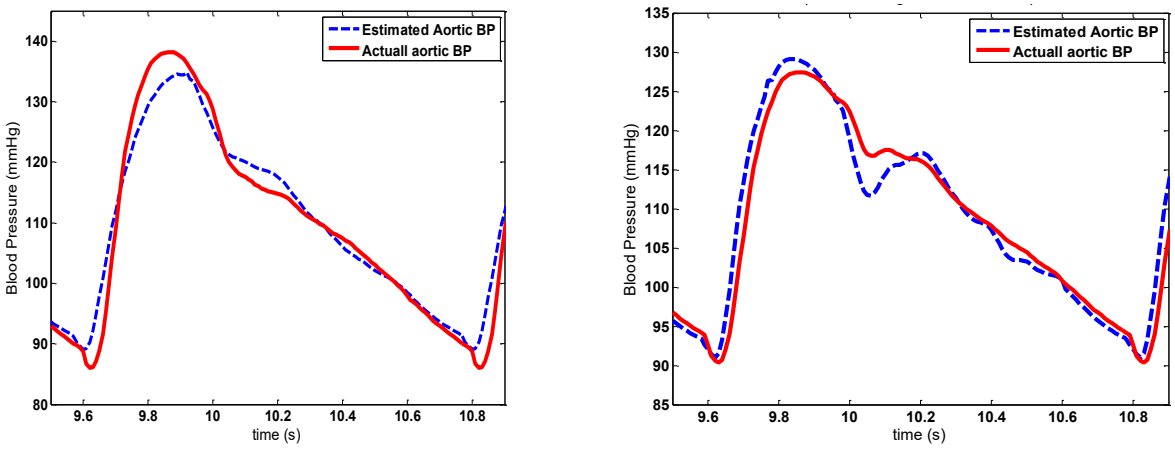

Figure 4–8 - Using tube-load model for reproducing the aortic blood pressure in case of (a) Arterial stiffening and (b) PAD in lower extremities.

Table 4-3 – Tube-load model parameters of the arterial stiffening simulations.

Simulation	$K = (\frac{Eh}{r})/(\frac{Eh}{r})_{Normal}$	*PTT*	$\alpha = Z_C C_P$ *1000	$\beta = Z_C/R_P$	*RMSE (mm Hg)*
#0 (Normal Arterial Tree)	1	0.169	15.913	0.845	1.011
#1	1.2	0.157	28.244	0.935	1.294
#2	1.4	0.148	38.572	1.013	1.561
#3	1.6	0.141	47.362	1.082	1.789
#4	1.8	0.135	55.431	1.146	1.982
#5	2.0	0.130	62.667	1.204	2.136

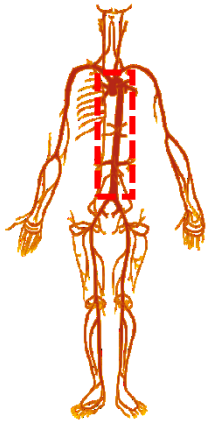

Simulation summary:

Affected arteries: The ascending aorta and abdominal aorta.

$$\frac{Eh}{r_o} = K * C_1 \exp(C_2 . r_o) + K * C_3$$

K: arterial stiffening index

Figure is adapted from [24].

Table 4-4 - Tube-load model parameters of the femoral atherosclerotic blockage simulations[3].

Simulation	*Blockage area (%)*	*Length (cm)*	*PTT (mS)*	*$\alpha=Z_C C_P$ *1000*	*$\beta=Z_C/R_P$*	*RMSE (mm Hg)*
#0 (Normal Arterial Tree)	0	0	0.169	15.913	0.845	1.011
#1	30%	2	0.169	13.033	0.843	0.954
#2	30%	4	0.169	10.760	0.838	0.907
#3	30%	6	0.169	9.103	0.833	0.876
#4	30%	8	0.170	6.889	0.825	0.854
#5	30%	10	0.170	5.924	0.820	0.842
#6	50%	2	0.169	8.630	0.838	0.864
#7	50%	4	0.170	2.873	0.820	0.845
#8	50%	6	0.170	0.010	0.801	0.924
#9	50%	8	0.169	0.010	0.781	1.066
#10	50%	10	0.168	0.010	0.763	1.212

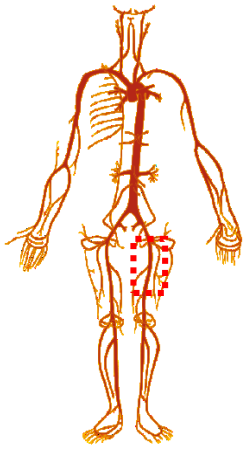

Figure is adapted from [24].

Simulation summary:

Affected arteries: The femoral.

$$Blockage\ area\ \% = \frac{A_S}{A_0}\%$$

$$A_0 = \pi {r_o}^2$$

$$A_S = \pi({r_o}^2 - {r_S}^2)$$

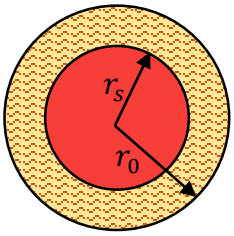

r_o: *radius of the normal*

r_S: *radius of the lumen in the existance blockage*

In the Figure 4–9 (d),(e) and (f) parameters α, β and PTT for PAD blockage are shown. These values are shown with respect of the area blockage and the length of the blockage. As shown in these figures, with the increase of the length of the blockage or the area of blockage, the PTT does not change noticeably (± 1 mS) while the value of α and β decrease.

[3] The complete sets of simulation are presented in the appendix-B.

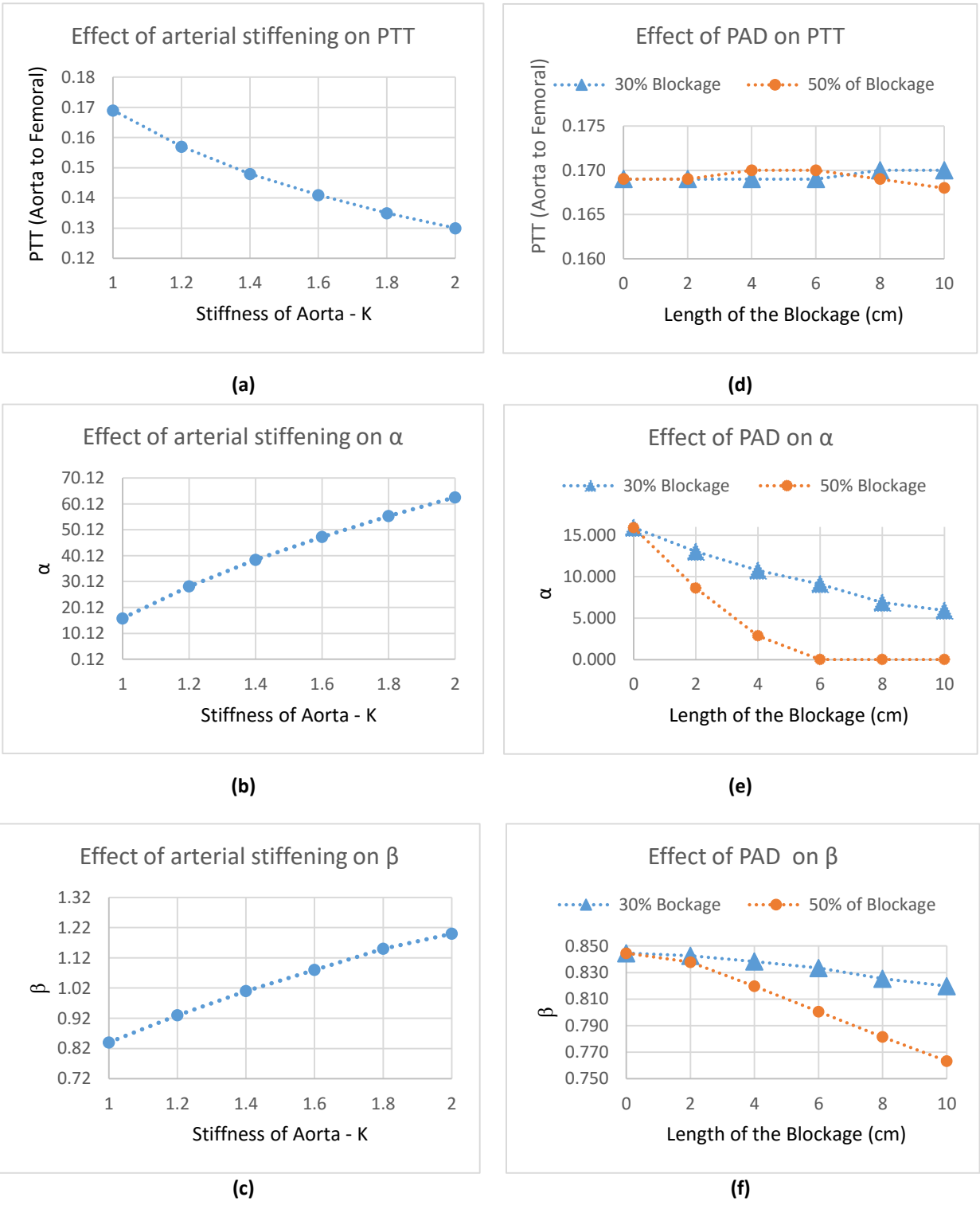

Figure 4–9- Effect of arterial diseases on the tube-load mode parameters: Arterial stiffening on (a) PTT, (b) α and (c) β, Peripheral artery disease on (d) PTT, (e) α and (f) β.

The qualitative analysis of the change in the parameters of the tube-load model for these simulations is summarized in the Table 4-5. This table show the agreement between the result of simulations and the expectated change.

Table 4-5 - The effect of arterial diseases on the tube-load model parameters, the expectation versus the simulation result.

Parameters	Arterial Stiffening		Atherosclerotic Blockage	
	Expectation	*Simulation result*	*Expectation*	*Simulation result*
PTT	↓	↓	Unchanged	Unchanged
α	↑	↑	↓	↓
β	↑	↑	↓	↓

4.5.1 Diagnostic procedure

The suggested procedure of diagnosis of PAD and arterial stiffening based on the new method is shown in the Error! Reference source not found..

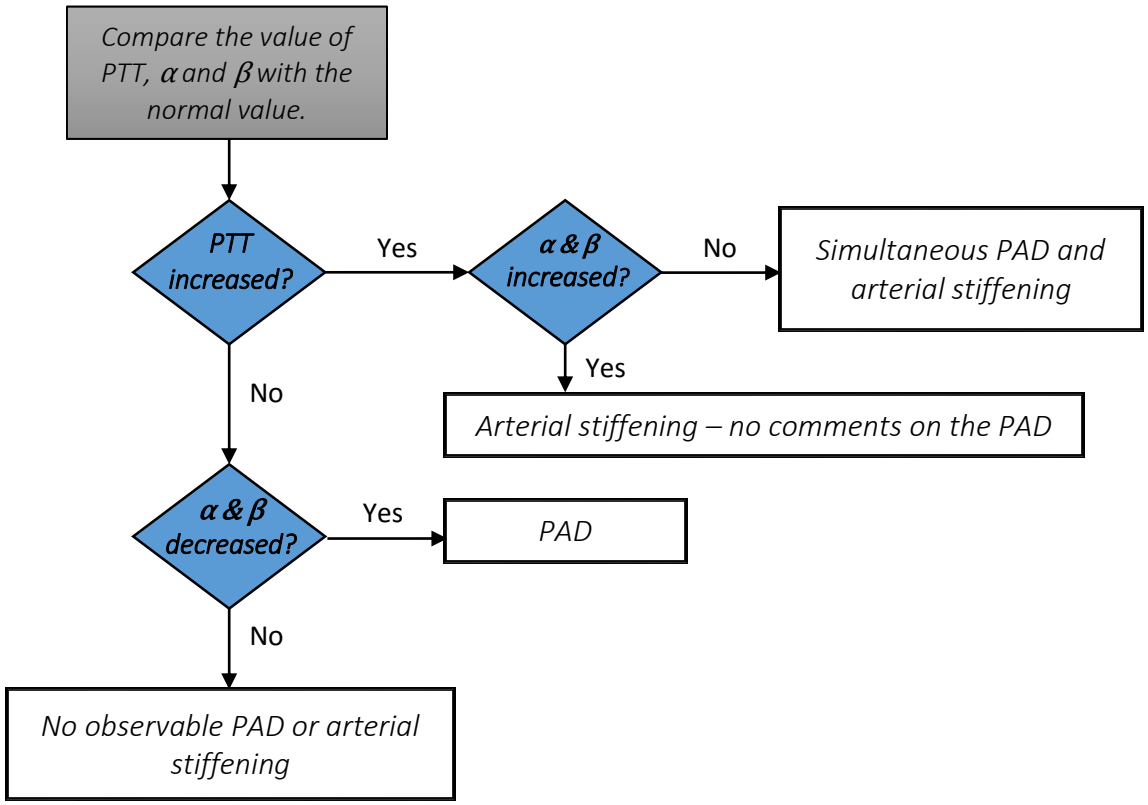

Figure 4–10 - The procedure of diagnosis arterial diseases based on the tube-load model parameters.

As this chart suggests, first the PTT needs to be checked. If there is no change in the value of PTT, the parameters have to be checked for detecting PAD. When the PTT shows decrease while α and β decrease or stay unchanged, it might indicate PAD and arterial stiffening in the arteries. However, if the parameters α and β increase there might or might not be PAD in the lower extremities.

4.6- Discussion

4.6.1 Validity of Tube-Load Model as Representation of Arterial Tree with CVD

In this paper, the parameters of the tube-load model were used to detect CVD whitin the arterial tree. To evaluate these parameters, first the tube-load model was used to estimate the aortic blood pressure in simulated subjects with CVD condition. The results show that the error of the tube-load model in reproducing the blood pressure at aorta, was less than 1.2 (mmHg) in all of the PAD and arterial stiffening simulations, while the total change in the pressure in these cases is between 50 to 80 (mmHg). These results validated the efficiency of the tube-load model in simulated cases of arterial trees with CVD conditions.

4.6.2 The Validity of the CVD Diagnostic Method based on the Tube-Load Model

The main goal of this work was to develop a novel method for primary diagnosis of PAD. This model is based on the parameters of a mathematical model of the arterial tree, namely tube-load model. To develop the method, first the effects of PAD on the characteristics of the arterial tree were determined and then, based on the definition of the parameters of the tube-load model, the expected trend of change in the parameters were evaluated. In order to validate the method, different types of PAD, with different length and cross-section were simulated. Based on the result of the simulation was shown in the Table 4-3, Table 4-4 and Table 4-5, the overall trend of change in the parameters of the simulated cases, met the criteria for detecting the abnormal changes associated with different diseases.

One of the other open questions up to this point, is the behavior of the diagnostic parameters, namely α, β and PTT, in cases that arterial stiffening and PAD develop at the same time.

One of the assumptions of this work includes having access to aortic blood pressure. However, it is well-known that the measurement of aortic blood pressure is highly invasive. Therefore, this waveform needs to be replaced either by aortic flow, or carotid pressure waveform in order to be able to use this approach more broadly, which can be one of the future works of this project.

4.6.3 Diagnosis CVD via Using Tube-Load Model versus other Available Methods

The procedure of diagnosis of PAD and arterial stiffening using the new method was shown in the Figure 4–10. The proposed method uses a comparative method to determine the abnormalities in the arterial tree, in other word, the estimated parameters at each measurement, will be compared to the one of the normal blood pressure.

This makes the method more accurate and independent from the results of other patients. On the other hand, since the method requires access to the normal blood pressure waveforms, at this stage, it can only be used for patients who do a regular checkup. While in case of PAD, other methods of diagnosis such as ABI and FMD tests, provide an overall evaluation at each measurement.

While the ABI is less sensitive for diagnosis of mild PAD [6], the tube-load model, is able to easily detect a small blockages of 50% cross-sectional blockage and 2 cm length, with more than 45% of change in parameter α. One the other advantages of this model, over the ABI, is in the case simultaneous PAD at upper and lower extremities. In this case, the systolic may increase in a way that the ration stays the same, while the tube-load approach uses two different tubes, upper and lower tube for diagnose PAD at each section.

Moreover, while the risk assessment method provides a general score of the probability of having PAD, the tube-load model approach help the medical staff to detect PAD with higher accuracy.

FMD test, uses the hypothesis of the effect of the atherosclerosis on the endothelial function of the artery to determine the systemic atherosclerosis. Tube-load model approach in comparison with FMD test, does not require any test preparation, such as fasting, or other limitations and provide specific information on PADs.

In terms of diagnosis the arterial stiffness, the method provides an automatic instant

measurement of PTT which has been shown to be very effective in the diagnosis of arterial stiffening. While other methods of measuring PTT usually involve foot-to-foot measurement.

4.7- Conclusion

In this paper, the possibility of using tube-load model parameters for detecting arterial diseases was examined and validated. Based on the analysis on the result of simulations of arterial stiffening and PAD, the method shows promising result in detecting PAD blockages and stiffened arteries. In the future, the model may also be applied for detecting other types of diseases of the arterial tree.

4.8- References

[1] S. Mendis, P. Puska, and B. Norrving, "Global atlas on cardiovascular disease prevention and control," *World Heal. Organ.*, pp. 2–14, 2011.

[2] D. P. Zipes and H. J. J. Wellens, "Sudden Cardiac Death," *Circulation*, vol. 98, no. 21. pp. 2334–2351, 1998.

[3] W. S. Weintraub, S. R. Daniels, L. E. Burke, B. a. Franklin, D. C. Goff, L. L. Hayman, D. Lloyd-Jones, D. K. Pandey, E. J. Sanchez, A. P. Schram, and L. P. Whitsel, "Value of primordial and primary prevention for cardiovascular disease: A policy statement from the American Heart Association," *Circulation*, vol. 124, no. 8, pp. 967–990, 2011.

[4] S. M. Grundy, T. Bazzarre, J. Cleeman, R. B. D'Agostino, M. Hill, N. Houston-Miller, W. B. Kannel, R. Krauss, H. M. Krumholz, R. M. Lauer, I. S. Ockene, R. C. Pasternak, T. Pearson, P. M. Ridker, and D. Wood, "Prevention Conference V: Beyond secondary prevention: identifying the high-risk patient for primary prevention: medical office assessment: Writing Group I.," *Circulation*, vol. 101, no. 1, pp. E3–E11, 2000.

[5] L. Norgren, W. R. Hiatt, J. a. Dormandy, M. R. Nehler, K. a. Harris, F. G. R. Fowkes, and R. B. Rutherford, "Inter-Society Consensus for the management of peripheral arterial disease (TASC II)," *Int. Angiol.*, vol. 26, no. 2, pp. 82–157, 2007.

[6] S. a Carter, "Indirect systolic pressures and pulse waves in arterial occlusive diseases of the lower extremities.," *Circulation*, vol. 37, no. 4, pp. 624–637, 1968.

[7] S. C. Nam, S. H. Han, S. H. Lim, Y. S. Hong, J. H. Won, J. I. Bae, and J. Jo, "Factors affecting the validity of ankle-brachial index in the diagnosis of peripheral arterial obstructive disease.," *Angiology*, vol. 61, no. 4, pp. 392–396, 2010.

[8] M. Charakida, S. Masi, T. F. Lüscher, J. J. P. Kastelein, and J. E. Deanfield, "Assessment of

atherosclerosis: The role of flow-mediated dilatation," *Eur. Heart J.*, vol. 31, no. 23, pp. 2854–2861, 2010.

[9] G. Zhang, J. O. Hahn, and R. Mukkamala, "Tube-load model parameter estimation for monitoring arterial hemodynamics," *Front. Physiol.*, vol. 2 NOV, no. November, pp. 1–18, 2011.

[10] M. Rashedi, N. Fazeli, a Chappell, S. Wang, R. MacArthur, M. S. McMurtry, B. a Finegan, and J. O. Hahn, "Comparative Study on Tube-Load Modeling of Arterial Hemodynamics in Humans," *ASME J. Biomech.*, vol. 135, no. March, p. 31005, 2013.

[11] C. R. Ethier and C. A. Simmons, "Introductory Biomechanics - from Cells to Organisms," *Book*, p. 545, 2007.

[12] F. M. White, "Fluid Mechanics," *McGraw-Hill*, p. 1024, 2009.

[13] S. Laurent, J. Cockcroft, L. Van Bortel, P. Boutouyrie, C. Giannattasio, D. Hayoz, B. Pannier, C. Vlachopoulos, I. Wilkinson, and H. Struijker-Boudier, "Expert consensus document on arterial stiffness: Methodological issues and clinical applications," *Eur. Heart J.*, vol. 27, no. 21, pp. 2588–2605, 2006.

[14] G. Gamble, J. Zorn, G. Sanders, S. MacMahon, and N. Sharpe, "Estimation of arterial stiffness, compliance, and distensibility from M-mode ultrasound measurements of the common carotid artery.," *Stroke.*, vol. 25, no. 1, pp. 11–16, 1994.

[15] N. Stergiopulos, B. E. Westerhof, and N. Westerhof, "Total arterial inertance as the fourth element of the windkessel model.," *Am. J. Physiol.*, vol. 276, no. 1 Pt 2, pp. H81–H88, 1999.

[16] M. F. O'Rourke, J. a. Staessen, C. Vlachopoulos, D. Duprez, and G. E. Plante, "Clinical applications of arterial stiffness; definitions and reference values," *Am. J. Hypertens.*, vol. 15, no. 5, pp. 426–444, 2002.

[17] Z. Sun, "Aging, Arterial Stiffness, and Hypertension," *Hypertension*, vol. 65, no. 2, pp. 252–256, 2014.

[18] F. U. S. Mattace-Raso, T. J. M. Van Der Cammen, A. Hofman, N. M. Van Popele, M. L. Bos, M. a D. H. Schalekamp, R. Asmar, R. S. Reneman, A. P. G. Hoeks, M. M. B. Breteler, and J. C. M. Witteman, "Arterial stiffness and risk of coronary heart disease and stroke: The Rotterdam Study," *Circulation*, vol. 113, no. 5, pp. 657–663, 2006.

[19] O. Vardoulis, T. G. Papaioannou, and N. Stergiopulos, "On the Estimation of Total Arterial Compliance from Aortic Pulse Wave Velocity," *Ann. Biomed. Eng.*, vol. 40, no. 12, pp. 1–8, 2012.

[20] B. M. Pannier, A. P. Avolio, A. Hoeks, G. Mancia, and K. Takazawa, "Methods and devices for measuring arterial compliance in humans," *Am. J. Hypertens.*, vol. 15, no. 8, pp. 743–753, 2002.

[21] M. S. Olufsen, C. S. Peskin, W. Y. Kim, E. M. Pedersen, A. Nadim, and J. Larsen, "Numerical simulation and experimental validation of blood flow in arteries with structured-tree outflow conditions," *Ann. Biomed. Eng.*, vol. 28, no. 11, pp. 1281–1299, 2000.

[22] M. S. Olufsen, "Structured tree outflow condition for blood flow in larger systemic arteries.," *Am. J. Physiol.*, vol. 276, no. 1 Pt 2, pp. H257–H268, 1999.

[23] A. A. Laogun and R. G. Gosling, "In vivo arterial compliance in man.," Clin. Phys. Physiol. Meas., vol. 3, no. 3, pp. 201–212, 1982.

[24] "Arterial system." [Online]. Available: https://commons.wikimedia.org/wiki/File:Arterial_System_-_complete.svg.

5. Sensitivity of Tube-Load Model to PAD Severity

Previously in chapter 4 the ability of the tube-load model for detecting atherosclerotic blockage in the extremities was discussed and validated. In this chapter, a further step will be taken toward investigating the sensitivity of the tube-load model parameter to size of a single blockage in the femoral artery.

5.1- Introduction

Peripheral artery disease (PAD) is one of the most prevalent types of the cardiovascular diseases (CVDs) that approximately affect 8 to 12 million people in the United States [1]–[3]. PAD blockages asymptomatically grow in the peripheries and do not become symptomatic till late stages. Symptomatic PAD may cause pain fatigue and in advanced cases may lead to amputation [4]–[6]. Furthermore, the existence of PAD may be a symptom of systemic atherosclerosis [5], [3], [7]. There are many methods for preliminary diagnosis of PAD, including ankle brachial index, flow mediated dilatation test and risk assessment method [5], [8]–[12].

Another method for diagnosis of PAD is using the "tube-load" model which is a mathematical mode of the arterial tree. The parameters of the tube-load model have physiological meaning. It was previously shown that the parameters of the tube-load model are sensitive to the existence of PAD blockage in lower extremities (refer to Chapter 4).

In this chapter, by using parameters analysis, further investigation is done to assess the sensitivity of the parameters of the tube-load model to the geometry of the blockage.

5.2- Background

5.2.1 Peripheral Artery Disease (PAD)

Peripheral artery disease defines the growth of atherosclerotic blockages in the peripheries, usually at the lower extremities [3], [13]. PAD blockages or stenosis narrow down the luminal area of the arteries, resulting in an increase of the resistance in the artery to the blood flow.

Based on the Hegan-Poiseuillie law, for a laminar flow of a incompressible, Newtonian fluid, the resistance of a circular tube to the flow can be calculated based on the pressure drop as follows. For a circular tube with the length l and radius r, the resistance applied to the flow a fluid with viscosity μ , can be estimated by the following equation:

$$R = \frac{8\mu l}{\pi r^4} \tag{5-1}$$

Therefore, for a stenosis in the artery, the resistance can be estimated using the equation (5-1) by replacing the length and the radius of the stenosis and the viscosity of the blood. Since the value of $8\mu/\pi$ is constant for each single arterial system, it can be concluded that the resistance of the stenosis and its geometry are related as $R \propto l/r^4$. In this chapter, this parameter is referred as the severity index, defined as $\gamma = l/r^4$. However, it should be noted that the expression "severity" used in this context does not necessarily have the same meaning as in medical applications.

5.2.2 Tube-Load Model

Tube-load model, is a mathematical model of the arterial tree. One type of the tube-load model is shown in Figure 5-1. This model uses a few parameters including the characteristic impedance (Z_C), peripheral resistance (R_P), peripheral compliance (C_P) and pulse transit time (PTT) to simulate the behavior of the cardiovascular system. Characteristic impedance, which is defined for the conduit artery, is described as $Z_c = \sqrt{\frac{l_{tube}}{C_{tube}}}$, whereas PTT can be modeled as $PTT = d_{tube}\sqrt{l_{tube}.C_{tube}}$. l_{tube} and C_{tube} are defined as follows:

$$l_{tube} = \int_0^L C_u \frac{\rho}{A(x)} dx \tag{5-2}$$

$$C_{tube} = E\frac{\pi L D^2}{2h} \tag{5-3}$$

The coefficient of C_u is used for non-flat velocity profile of the blood flow based on the Womersley's theory, ρ the density of blood and A the cross-section of the artery. E is the mean value of Young's modulus of the artery, L, D and h indicate the length, the diameter and the

thickness of the main artery respectively [14]–[16].

However, by having access to only the aortic and femoral blood pressure, not all the parameters of the tube-load model are identifiable. In fact, the values of three parameters, namely $\alpha = Z_C C_P$, $\beta = Z_C/R_P$ and PTT are identifiable (refer to Chapter 4). In the next subsection, the effect of PAD on these parameters will be determined and discussed.

5.2.3 Effects of PAD on the Tube-Load Model Parameters

When the arterial system is subjected to PAD, the aorta-femoral tube would not be affected. Therefore in the main artery, the inertance (l_{tube}) and the compliance (C_{tube}) would not be affected and therefore, Z_c will remain unchanged, while the peripheral resistance (R_P) is known to increase.

This change may be observable in the parameter β which is a function of the peripheral resistance. The value of β for a normal arterial tree versus the same arterial tree when it is subject to stenosis, is formulated as follows:

$$\frac{\beta_1}{\beta_0} = \frac{Z_{C_1}}{Z_{C_0}} . \frac{R_{P_0}}{R_{P_1}} \tag{5-4}$$

in which the index 1, shows a arterial system with stenosis disease, while index 0 is the normal system. Since $Z_{C_1} = Z_{C_0}$, as it was discussed above, this equation can be rewritten as follows:

$$\frac{R_{P_1}}{R_{P_0}} = \frac{\beta_0}{\beta_1} \tag{5-5}$$

This equation basically means that the value of β is proportional to the total resistance of the peripheries. In the following sections, this relation will be first validated by using the flow information of an arteria tree the simulator and applying the Windkessel theory.

Moreover, the resistance will be analysed to check the sensitivity of the parameters of the tube-load model to the severity index of a single blockage.

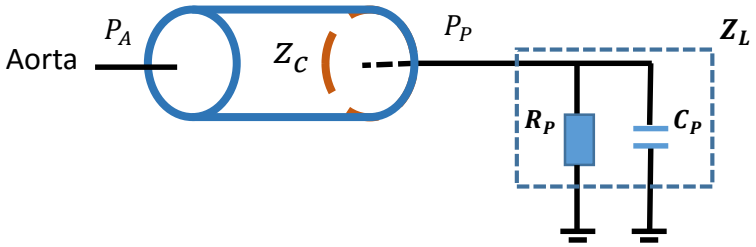

Figure 5-1 – Tube-load model.

5.3- Method

5.3.1 Simulating PAD

In order to validate the equation (5-5), first different cases of femoral blockage were simulated in a high-fidelity model of the arterial tree, described in the Appendix-B [17], [18].

These simulation covered mild to severe PADs with 30% to 70% of cross-sectional blockage in luminal area and the length of 2 to 10 cm. Afterwards, by exporting the blood pressure waveforms of the aorta and of the femoral, the parameters of the tube-load model were determined (the procedure is described in Chapter 4).

5.3.2 Windkessel Theory vs. Tube-Load Model Estimation of Peripheral Resistance

According to the Windkessel theory, the resistance of a compliant artery which is modeled as a flexible tube, can be calculated using the flow and pressure data. If the peripheral arteries are considered as a single tube, based on the Windkessel model the resistance can be estimated as follows:

$$R_P = \frac{\bar{P}_p}{\bar{Q}_p} \tag{5-6}$$

Therefore, the peripheral resistance of each of the simulations, can be calculated by measuring the mean flow and the pressure in a complete cycle of the heart. Considering this, the resistance in case of PAD versus the one for a normal artery can be calculated as follows:

$$\frac{R_{P_1}}{R_{P_0}} = \frac{\bar{P}_{p_1}}{\bar{Q}_{p_1}} \frac{\bar{Q}_{p_0}}{\bar{P}_{p_0}} \tag{5-7}$$

Equations (5-7) and (5-5), give two approaches to calculate the resistance of two different simulation cases. Since equation (5-7) directly uses the flow data of the arterial system, it can be used for validating equation (5-5).

5.3.3 Sensitivity of Tube-Load Model Parameter to the Severity Index

PAD, as an obstacle in the arteries, adds resistance to the system. If the peripheral resistance of a healthy system is shown with R_{P_0}, the one of a system with PAD is shown with R_{P_1} and the resistance associated to the stenosis for that case is indicated by R_{s_1}, the R_{P_1} can be approximately written as follows:

$$R_{P_1} \simeq R_{P_0} + R_{s_1} \tag{5-8}$$

Therefore, R_{P_0} and R_{P_1} are related as follows:

$$\frac{R_{P_1}}{R_{P_0}} \simeq \frac{R_{P_0} + R_{s_1}}{R_{P_0}} \tag{5-9}$$

$$\frac{R_{P_1}}{R_{P_0}} \simeq 1 + \frac{R_{s_1}}{R_{P_0}} \tag{5-10}$$

Comparing the last equation with equation (5-5), the following equation is found;

$$\frac{\beta_0}{\beta_1} \simeq 1 + \frac{R_{s_1}}{R_{P_0}} \tag{5-11}$$

Therefore, the resistance of the stenosis is estimated as shown:

$$R_{s_1} \simeq R_{P_0}\left(\frac{\beta_0}{\beta_1} - 1\right) \tag{5-12}$$

As it was mentioned before, the stenosis resistance is proportional to the severity index: $R_{s_1} \propto \gamma$. On the other hand, the value of $R_{P_0}$is constant for each system of the arterial tree. Therefore,

$$\left(\frac{\beta_0}{\beta_1} - 1\right) \propto \gamma \tag{5-13}$$

This equation shows, not only the fact that the value of β is affected by the existence of a PAD

blockage but also the recognition that the change is proportional to the severity index. In order to validate this statement, for each of the simulations of different cases of PAD, the severity index and the parameter β were evaluated. Then by comparing the value of β for a normal case, $\left(\frac{\beta_0}{\beta_1}-1\right)$ was evaluated. The liner regression between $\left(\frac{\beta_0}{\beta_1}-1\right)$ and γ was conducted.

5.4- Result

5.4.1 Simulating PAD

In the Table 5-1, fifteen different cases of femoral stenosis and one simulation of a normal arterial tree is shown. The severity index ($\boldsymbol{\gamma}$) is also calculated for each of these simulations. In this table, the parameters of the tube-load model, α, β and PTT are also presented.

Table 5-1 – Simulation of femoral stenosis and tube-load model parameters.

Sim.	$r_s\ (cm)$	$l_s\ (cm)$	$\gamma/1000$	PTT	α*1000	β
Normal	0.36	-	-	0.17	15.83	0.85
1	0.30	2	0.25	0.17	12.74	0.84
2	0.30	4	0.49	0.17	10.33	0.84
3	0.30	6	0.74	0.17	8.59	0.83
4	0.30	8	0.99	0.17	7.18	0.83
5	0.30	10	1.23	0.17	6.15	0.82
6	0.25	2	0.51	0.17	8.09	0.84
7	0.25	4	1.02	0.17	2.98	0.82
8	0.25	6	1.54	0.17	0	0.8
9	0.25	8	2.05	0.17	0	0.78
10	0.25	10	2.56	0.17	0	0.76
11	0.20	2	1.25	0.17	0	0.81
12	0.20	4	2.50	0.17	0	0.75
13	0.20	6	3.75	0.16	0	0.70
14	0.20	8	5.00	0.16	0	0.66
15	0.20	10	6.25	0.16	0	0.63

5.4.2 Direct Measurement of Resistance versus Tube-Load Model Estimation

As discussed before, the resistance in the periphery can be directly calculated by using the mean

peripheral flow ($\bar{Q}_p$) and pressure ($\bar{P}_p$) within a cardiac cycle. Comparing the peripheral resistance of each simulation case to the peripheral resistance of the normal case, one can calculate the value of R_{P_1}/R_{P_0}.

On the other hand, as the equation (5-5) suggests, this ratio can also be estimated using the tube-load model parameters. By comparing the parameter β for each simulation to the one associated with the normal arterial tree β_0, the ratio of β_0/β can be calculated. For the simulations, described in the previous sections, the value of the parameters R_{P_1}/R_{P_0} and β_0/β are calculated and shown in the Table 5-2.

Table 5-2 – Determining the ratio of R_{P_1}/R_{P_0} using tube-load model versus direct measurement.

Sim.	$r_s\ (cm)$	$l_s\ (cm)$	$R_P = \bar{P}_p/\bar{Q}_p$	R_{P_1}/R_{P_0}	β	β_0/β
Normal	0.36	0	16.76	1.00	0.85	1.00
1	0.30	2	16.85	1.01	0.84	1.00
2	0.30	4	16.95	1.01	0.84	1.01
3	0.30	6	17.03	1.02	0.83	1.02
4	0.30	8	17.11	1.02	0.83	1.02
5	0.30	10	17.18	1.03	0.82	1.03
6	0.25	2	17.08	1.02	0.84	1.01
7	0.25	4	17.40	1.04	0.82	1.03
8	0.25	6	17.71	1.06	0.80	1.06
9	0.25	8	18.02	1.07	0.78	1.08
10	0.25	10	18.32	1.09	0.76	1.11
11	0.20	2	17.85	1.06	0.81	1.05
12	0.20	4	18.91	1.13	0.75	1.13
13	0.20	6	19.96	1.19	0.70	1.21
14	0.20	8	21.02	1.25	0.66	1.28
15	0.20	10	22.07	1.32	0.63	1.35

In order to compare the values of R_{P_1}/R_{P_0} and β_0/β, the ratio of each case are shown in Figure 5-2. In this figure, the ability of the parameters of the tube-load model to track the change in the peripheral resistance is exhibited.

In order to evaluate the agreement between these two methods for estimating the value of the peripheral resistance, the Bland-Altman method which is an alaysis for determining the agreement

between two different method, was found for the simulations presented in the Table 5-2. The result is shown in the Figure 5-3. As can be verified in this figure, for these simulations, the difference between these two methods lied withint 95% limits of agreement.

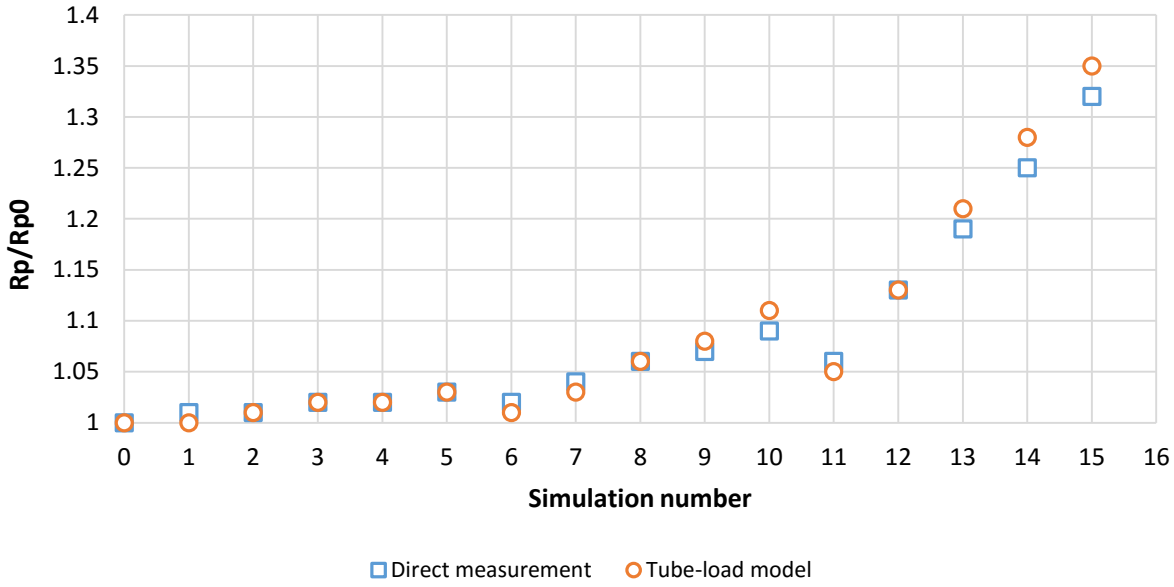

Figure 5-2 – Using the tube-load model parameters to estimate the change in the resistance in case of femoral atherosclerosis associated with PAD.

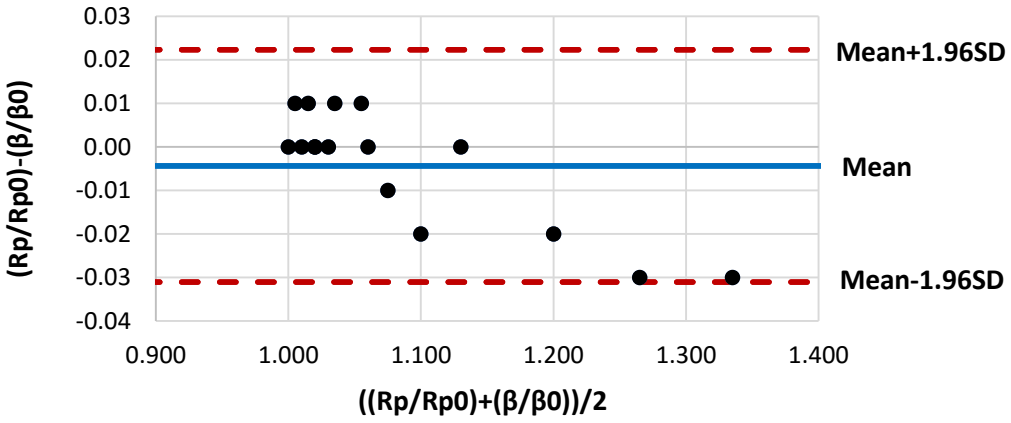

Figure 5-3 – Limits of agreement (based on the Bland-Altman method) between direct measurement of the peripheral resistance versus using the parameters of the tube-load model.

5.4.3 Sensitivity of Tube-Load Model Parameter to the Severity Index

According to the equation (5-13), if the parameter β of an arterial tree with PAD is compared to the one of the normal cardiovascular system, and the value of $(\beta_0/\beta - 1)$ is calculated for that case, it is expected to be proportional to the severity index of that blockage γ.

For the simulations shown in the Table 5-1, the value of γ and β are calculated and shown. Using the information provided on that table, the value of $(\beta_0/\beta - 1)$ can be evaluated. The result is shown in the Table 5-3.

In order to examine the proportionality of $(\beta_0/\beta - 1)$ to the severity index (γ) for the fifteen different cases described in the Table 5-3, linear regression analysis was performed. The linear trend line versus the actual result is shown in the Figure 5-4. The intercept of the trend line was set to 0, to resemble the normal case, at which both value equal zero. The coefficient of determination for the simple linear regression was $R^2 = 0.98$, which states a high fidelity.

Table 5-3 – Determining the sensitivity of tube-load model to the severity index.

Sim.	$r_s\ (cm)$	$l_s\ (cm)$	$\gamma/1000$	β	β0/β -1
Normal	0.364	0	0.00	0.85	0.00
1	0.3	2	0.25	0.84	0.00
2	0.3	4	0.49	0.84	0.01
3	0.3	6	0.74	0.83	0.02
4	0.3	8	0.99	0.83	0.02
5	0.3	10	1.23	0.82	0.03
6	0.25	2	0.51	0.84	0.01
7	0.25	4	1.02	0.82	0.03
8	0.25	6	1.54	0.80	0.05
9	0.25	8	2.05	0.78	0.08
10	0.25	10	2.56	0.76	0.10
11	0.2	2	1.25	0.81	0.05
12	0.2	4	2.50	0.75	0.11
13	0.2	6	3.75	0.70	0.17
14	0.2	8	5.00	0.66	0.22
15	0.2	10	6.25	0.63	0.26

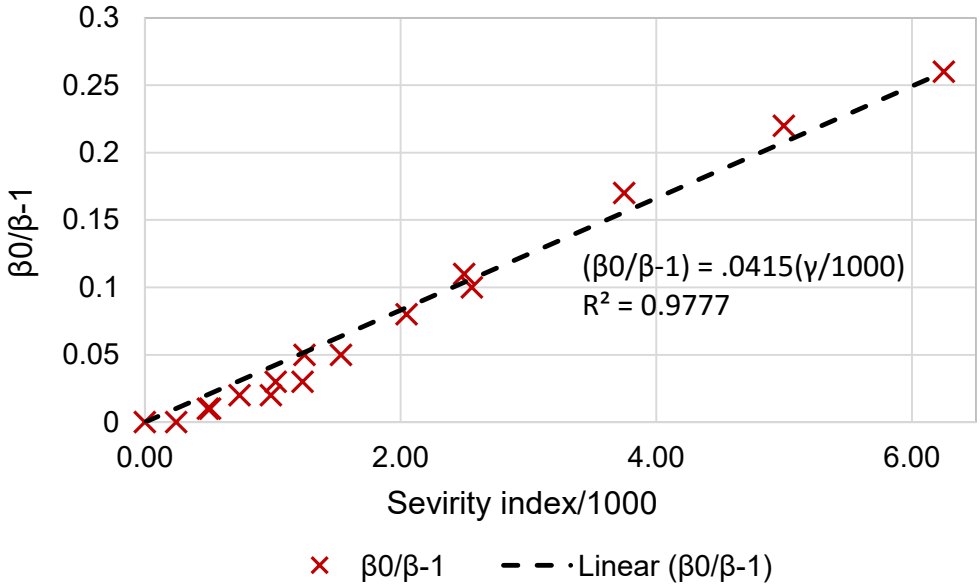

Figure 5-4 – Proportionality of the $(\boldsymbol{\beta_0/\beta - 1})$ and severity index $\boldsymbol{\gamma}$ in PAD simulations.

5.5- Discussion

5.5.1 Ability of Tube-Load Model to Detect Arterial Blockage in the Extremities

It was previously discussed that the parameters of the tube-load model, reflect many features of the arterial tree, including the one that are affected by diseases such as PAD (refer to chapter 4). In this study, the effect of PAD was further examined. To further study these parameters, fifteen different cases of femoral stenosis were simulated. Based on the analysis on the tube-load model parameters of these simulations, it was observed that not only parameters of the tube-load model (specifically β) are affected by the existence of the PAD, but also the size of the size of the PAD blockage is reflected in the change of the parameters.

5.5.2 Using the Tube-Load Model to Estimate the Change in the Resistance Associated with PAD

In this chapter, one of the parameters of the tube-load model, β was used to determine the change in the peripheral resistance, after growth of a PAD blockage. Another approach for determining the value of peripheral resistance is using the Windkessel model theory. Based on this theory the

resistance was calculated from the analysis of the flow and pressure (Figure 5-2). This approach can be used to check the ability of the tube-load model to estimate the change of the value of peripheral resistance. By examining the limits of agreement between two methods, it was observed that the confidence interval is very tight (Figure 5-3).In other words, tube-load model parameter is able to accurately estimate the change in the resistance associated with PAD, without having access to any information regarding the flow information.

5.5.3 Sensitivity of Tube-Load Model to the Severity of PAD Blockage

In this chapter, the effect of increase of the severity index associated with the size of PAD blockage, on one of the parameters of the tube-load model (β) was studied. According to the result of the simulations, the simple linear regression analysis between the severity index and the value of $(\beta_0/\beta - 1)$, showed that the parameters are proportional with the coefficient of determination of 0.98. This result suggests that this parameter is sensitive and proportional to the severity index.

5.6- Conclusion

In this chapter, the effects of the PAD blockage on the parameters of the tube-load model were discussed and examined. It was hypothesized that the parameter are sensitive to the geometry of blockages. This hypothesis was then validated using a high-fidelity model of arterial tree to simulate different cases of PADs in the femoral artery.

5.7- References

[1] F. G. Fowkes, E. Housley, E. H. Cawood, C. C. Macintyre, C. V Ruckley, and R. J. Prescott, "Edinburgh Artery Study: prevalence of asymptomatic and symptomatic peripheral arterial disease in the general population.," *Int. J. Epidemiol.*, vol. 20, no. 2, pp. 384–392, 1991.

[2] M. Criqui, A. Fronek, E. Barrett-Connor, M. Klauber, S. Gabriel, and D. Goodman, "The prevalence of peripheral arterial disease in a defined population.," *Circulation*, vol. 71, no. 3, pp. 510–515, 1985.

[3] A. T. Hirsch, M. H. Criqui, D. Treat-Jacobson, J. G. Regensteiner, M. A. Creager, J. W. Olin, S. H. Krook, D. B. Hunninghake, A. J. Comerota, M. E. Walsh, M. M. McDermott, and W. R. Hiatt, "Peripheral arterial disease detection, awareness, and treatment in primary care.," *JAMA*, vol. 286, no. 11, pp.

1317–1324, 2001.

[4] W. T. Meijer, A. W. Hoes, D. Rutgers, M. L. Bots, A. Hofman, and D. E. Grobbee, "Peripheral arterial disease in the elderly: The Rotterdam Study.," Arterioscler. Thromb. Vasc. Biol., vol. 18, no. 2, pp. 185–192, 1998.

[5] L. Norgren, W. R. Hiatt, J. a. Dormandy, M. R. Nehler, K. a. Harris, F. G. R. Fowkes, and R. B. Rutherford, "Inter-Society Consensus for the management of peripheral arterial disease (TASC II)," *Int. Angiol.*, vol. 26, no. 2, pp. 82–157, 2007.

[6] "About Peripheral Artery Disease (PAD)," *American Heart Association*. [Online]. Available: http://www.heart.org/HEARTORG/Conditions/More/PeripheralArteryDisease/About-Peripheral-Artery-Disease-PAD_UCM_301301_Article.jsp.

[7] A. T. Hirsch, S. L. Halverson, D. Treat-Jacobson, P. S. Hotvedt, M. M. Lunzer, S. Krook, S. Rajala, and D. B. Hunninghake, "The Minnesota Regional Peripheral Arterial Disease Screening Program: toward a definition of community standards of care.," *Vasc. Med.*, vol. 6, no. 2, pp. 87–96, 2001.

[8] G. Lawson, "The importance of obtaining ankle-brachial indexes in older adults: The other vital sign," *J. Vasc. Nurs.*, vol. 23, no. 2, pp. 46–51, 2005.

[9] S. Hyun, N. I. Forbang, M. a. Allison, J. O. Denenberg, M. H. Criqui, and J. H. Ix, "Ankle-brachial index, toe-brachial index, and cardiovascular mortality in persons with and without diabetes mellitus," *J. Vasc. Surg.*, vol. 60, no. 2, pp. 390–395, 2014.

[10] S. P. A. Nicolaï, L. M. Kruidenier, E. V Rouwet, M.-L. E. L. Bartelink, M. H. Prins, and J. A. W. Teijink, "Ankle brachial index measurement in primary care: are we doing it right?," *Br. J. Gen. Pract.*, vol. 59, no. 563, pp. 422–427, 2009.

[11] A. J. Flammer, T. Anderson, D. S. Celermajer, M. a. Creager, J. Deanfield, P. Ganz, N. M. Hamburg, T. F. Lüscher, M. Shechter, S. Taddei, J. a. Vita, and A. Lerman, "The assessment of endothelial function: From research into clinical practice," *Circulation*, vol. 126, no. 6, pp. 753–767, 2012.

[12] R. B. D'Agostino, R. S. Vasan, M. J. Pencina, P. a. Wolf, M. Cobain, J. M. Massaro, and W. B. Kannel, "General cardiovascular risk profile for use in primary care: The Framingham heart study," *Circulation*, vol. 117, no. 6, pp. 743–753, 2008.

[13] S. Mendis, P. Puska, and B. Norrving, "Global atlas on cardiovascular disease prevention and control," *World Heal. Organ.*, pp. 2–14, 2011.

[14] G. Gamble, J. Zorn, G. Sanders, S. MacMahon, and N. Sharpe, "Estimation of arterial stiffness, compliance, and distensibility from M-mode ultrasound measurements of the

common carotid artery.," *Stroke.*, vol. 25, no. 1, pp. 11–16, 1994.

[15] N. Stergiopulos, B. E. Westerhof, and N. Westerhof, "Total arterial inertance as the fourth element of the windkessel model.," *Am. J. Physiol.*, vol. 276, no. 1 Pt 2, pp. H81–H88, 1999.

[16] G. Zhang, J. O. Hahn, and R. Mukkamala, "Tube-load model parameter estimation for monitoring arterial hemodynamics," *Front. Physiol.*, vol. 2 , November, pp. 1–18, 2011.

[17] M. S. Olufsen, C. S. Peskin, W. Y. Kim, E. M. Pedersen, A. Nadim, and J. Larsen, "Numerical simulation and experimental validation of blood flow in arteries with structured-tree outflow conditions," *Ann. Biomed. Eng.*, vol. 28, no. 11, pp. 1281–1299, 2000.

[18] M. S. Olufsen, "Structured tree outflow condition for blood flow in larger systemic arteries.," *Am. J. Physiol.*, vol. 276, no. 1 Pt 2, pp. H257–H268, 1999.

6. Conclusion and Future work

6.1- Conclusion

In this project, a mathematical model of the arterial tree, namely a "tube-load model" was introduced as a potential basis for detecting abnormalities in the arterial tree. Examples of such abnormalities are the cardiovascular diseases (CVDs) which may affect the characteristics of the heart and the arteries. The emphasis of this project was on the diseases compromising the functionality of the arteries, with specific focus on the arterial stiffening of the aorta and the peripheral artery diseases (PADs) in the lower extremities.

By applying the inverse modeling of the tube-load model into two blood pressure waveforms of the system, namely: at the aorta and at the peripheral site, the parameters of the tube–load model can be identified. It was suggested that if we compare the parameters of a healthy arterial system, with the ones of the same system under a CVD condition, we can detect the changes associated with the diseases.

First, the effects of the diseases on the cardiovascular system were studied to determine the effects of the diseases on the tube-load model parameters. The expectation from the effect of the diseases on the tube-load model parameter was then used as the criteria for diagnosis.

In order to validate these hypotheses, one of the arterial tree models, which has been proved to be accurate was used to study the effects of the diseases on the arterial tree. In this model, different cases of PAD and arterial stiffening with different stages of severity, along with a normal case of a healthy arterial tree were simulated.

For each of these cases, the tube-load model parameters were evaluated and compared with the ones of the normal arterial tree. The result showed a high agreement with the expectation of the change in the parameters in both arterial stiffening cases and the PAD cases, which validated the method proposed in this thesis. However, in some cases of simulations of PAD, specifically in the ones representing late stages of the diseases, the changes in parameters were not proportional to the severity of the case. Nevertheless, based on the result of simulations, unlike other diagnosis

method, the model is able to even detect mild cases of PAD.

In cases of arterial stiffening, the model is able to give an instant value of the PTT, which can be used to estimate the stiffness of the aorta. The value of PTT can also be compared with the value of these parameter provided in the literature to evaluate the general description of the state of the patient.

Moreover, the effect of the peripheral artery disease on the value of the peripheral resistance was studied. Then the possibility of using the tube-load model to track than change was evaluated and validated with the value of the direct measurements. The result suggest high accuracy of the tube-load model to track the change of resistance in the downstream.

One of the interesting interpretations from the results of these models is that even though we do not have access to any information below the point of measurement in the femoral artery, the model can detect blockages in the extremities. In fact, the model is able to bring light into the parts of the arteries that we do not have access to, such as the aorta and the peripheries.

In conclusion, the approach introduced in this thesis provides a new method for primary diagnosis of the introduced diseases, which can be used along with the other methods or an independent marker of PAD and arterial stiffening.

6.2- Future work

Up to this point, it was shown that the tube-load model provided a promising result in terms of diagnosis arterial stiffening and PAD in lower extremities. However the functionality of this method has not been used in actual patients. It is also suggested that studying the behavior of these parameters in population, may lead to finding a normal range for the value of them. Finding a normal range, may be helpful in terms of instant diagnosis of diseases.

At this early stage of the work, the pressure at the aorta was used as the input of the system. However measuring the aortic pressure is highly invasive to date, in order to be able to use the method, the pressure at the aorta, can either be replaced by the flow at the aorta or alternatively by the pressure at the carotid which both can be measured non-invasively.

Moreover, the same approach that was followed for the lower extremities in this project can easily be used for upper extremities by replacing the pressure at the femoral artery by the one on the brachial or radial pressure. This approach is helpful to diagnose PAD in upper extremities.

In this project, the main focus of the diagnosis was on the most common types of the CVDs, however the method can be also applied to other types of diseases such as aneurysm which is known to affect the aorta and abdominal aorta.

Last but not the least, is the possibility of using this method to provide a quantitative description of the severity of the PAD. It is well-known that the PAD result in the increase of the peripheral resistance and the parameter β, is a function of the peripheral resistance. Therefore, the change is this parameter may be proportional to the size of the PAD blockage.

Complete List of References

AlGhatrif, M. et al., 2013. Longitudinal trajectories of arterial stiffness and the role of blood pressure: The Baltimore longitudinal study of aging. *Hypertension*, 62(5), pp.934–941.

Anon, About Peripheral Artery Disease (PAD). *American Heart Association*. Available at: http://www.heart.org/HEARTORG/Conditions/More/PeripheralArteryDisease/About-Peripheral-Artery-Disease-PAD_UCM_301301_Article.jsp.

Anon, Arterial system. Available at: https://commons.wikimedia.org/wiki/File:Arterial_System_-_complete.svg.

Anon, Blood circulation. Available at: http://clogged-arteries.howthingis.com/heart-disease-articles/.

Anon, Duplex ultrasound. Available at: https://www.nlm.nih.gov/medlineplus/ency/article/003433.htm.

Anon,The circulatory system. Available at: https://commons.wikimedia.org/wiki/File:Circulatory_System_en.svg#/media/File:Circulatory_System_no_tags.svg.

Avolio, a, 1980. Multi-branched model of the human arterial system. *Medical and Biological Engineering and Computing*, 18(6), pp.709–718. Available at: http://dx.doi.org/10.1007/BF02441895.

Bonel, H.M. et al., 2009. MR angiography of infrapopliteal arteries in patients with peripheral arterial occlusive disease by using Gadofosveset at 3.0 T: diagnostic accuracy compared with selective DSA. *Radiology*, 253(3), pp.879–890.

Bramwell, J.C. & Hill, a. V., 1922. The Velocity of the Pulse Wave in Man. *Proceedings of the Royal Society B: Biological Sciences*, 93(652), pp.298–306.

C.G. CARO, T.J. PEDLEY, R.C. SCHROTER, W.A.S., 1978. *The Mechanics of the Circulation*, oxford university press.

Carter, S. a, 1968. Indirect systolic pressures and pulse waves in arterial occlusive diseases of the lower extremities. *Circulation*, 37(4), pp.624–637.

Charakida, M. et al., 2010. Assessment of atherosclerosis: The role of flow-mediated dilatation. *European Heart Journal*, 31(23), pp.2854–2861.

Chobanian, A. V. et al., 2003. Seventh report of the Joint National Committee on Prevention, Detection, Evaluation, and Treatment of High Blood Pressure. *Hypertension*, 42(6), pp.1206–1252.

D'Agostino, R.B. et al., 2008. General cardiovascular risk profile for use in primary care: The Framingham heart study. *Circulation*, 117(6), pp.743–753.

Dalager, S. et al., 2008. Plaque in superficial femoral arteries indicates generalized atherosclerosis and vulnerability to coronary death: An autopsy study. *Journal of Vascular Surgery*, 47(2), pp.296–302.

Dong, J., Wong, K.K.L. & Tu, J., 2013. Hemodynamics analysis of patient-specific carotid bifurcation: A CFD model of downstream peripheral vascular impedance. *International Journal for Numerical Methods in Biomedical Engineering*, 29(4), pp.476–491. Available at: http://dx.doi.org/10.1002/cnm.2529.

Ethier, C.R. & Simmons, C.A., 2007. Introductory Biomechanics - from Cells to Organisms. *_Book*, p.545.

Farb, A. et al., 1995. Sudden coronary death. Frequency of active coronary lesions, inactive coronary lesions, and myocardial infarction. *Circulation*, 92(7), pp.1701–1709.

Flammer, A.J. et al., 2012. The assessment of endothelial function: From research into clinical practice. *Circulation*, 126(6), pp.753–767.

Fowkes, F.G. et al., 1991. Edinburgh Artery Study: prevalence of asymptomatic and symptomatic peripheral arterial disease in the general population. *International journal of epidemiology*, 20(2), pp.384–392.

Gamble, G. et al., 1994. Estimation of arterial stiffness, compliance, and distensibility from M-mode ultrasound measurements of the common carotid artery. *Stroke; a journal of cerebral circulation*, 25(1), pp.11–16.

Go, a. S. et al., 2014. Executive Summary: Heart Disease and Stroke Statistics--2014 Update: A Report From the American Heart Association. *Circulation*, 129(3), pp.399–410. Available at: http://circ.ahajournals.org/cgi/doi/10.1161/01.cir.0000442015.53336.12.

Goff, D.C. et al., 2014. 2013 ACC/AHA guideline on the assessment of cardiovascular risk: A report of the American college of cardiology/American heart association task force on practice guidelines. *Circulation*, 129(25 SUPPL. 1).

Greenwald, S.E., 2007. Ageing of the conduit arteries. *Journal of Pathology*, 211(2), pp.157–172.

Grundy, S.M. et al., 2000. Prevention Conference V: Beyond secondary prevention: identifying the high-risk patient for primary prevention: medical office assessment: Writing Group I. *Circulation*, 101(1), pp.E3–E11.

Hahn, J.O. et al., 2012. Subject-specific estimation of central aortic blood pressure using an individualized transfer function: A preliminary feasibility study. *IEEE Transactions on Information Technology in Biomedicine*, 16(2), pp.212–220.

Hahn, J.O., 2008. A system identification approach to non-invasive central cardiovascular monitoring, Thesis (Ph.D.)--Massachusetts Institute of Technology, Dept. of Mechanical Engineering, 2008.

Hirsch, A. T. et al., 2001. The Minnesota Regional Peripheral Arterial Disease Screening Program: toward a definition of community standards of care. *Vascular medicine (London, England)*, 6(2), pp.87–96.

Hirsch, a. T., 2001. Peripheral Arterial Disease Detection, Awareness, and Treatment in Primary Care. *JAMA: The Journal of the American Medical Association*, 286(11), pp.1317–1324.

Hirsch, A.T. et al., 2006. ACC/AHA 2005 Practice Guidelines for the Management of Patients With Peripheral Arterial Disease (Lower Extremity, Renal, Mesenteric, and Abdominal Aortic). *Circulation*, 113(11), pp.e463–e465.

Hyun, S. et al., 2014. Ankle-brachial index, toe-brachial index, and cardiovascular mortality in persons with and without diabetes mellitus. *Journal of Vascular Surgery*, 60(2), pp.390–395. Available at: http://dx.doi.org/10.1016/j.jvs.2014.02.008.

John, L.R., 2004. Forward electrical transmission line model of the human arterial system. *Medical & biological engineering & computing*, 42(3), pp.312–321.

Kelly, R. et al., 1989. Noninvasive determination of age-related changes in the human arterial pulse. *Circulation*, 80(6), pp.1652–1659.

Laogun AA, Gosling RG. In vivo arterial compliance in man. *Clin Phys Physiol Meas*. 1982;3(3):201-212. doi:10.1088/0143-0815/3/3/004.

Laurent, S. et al., 2006. Expert consensus document on arterial stiffness: Methodological issues and clinical applications. *European Heart Journal*, 27(21), pp.2588–2605.

Lawson, G., 2005. The importance of obtaining ankle-brachial indexes in older adults: The other vital sign. *Journal of Vascular Nursing*, 23(2), pp.46–51.

Lee, H.-Y. & Oh, B.-H., 2010. Aging and arterial stiffness. *Circulation journal : official journal of the Japanese Circulation Society*, 74(11), pp.2257–2262.

Lee, S.E. et al., 2008. Direct numerical simulation of transitional flow in a stenosed carotid bifurcation. *Journal of Biomechanics*, 41(11), pp.2551–2561.

Mattace-Raso, F.U.S. et al., 2006. Arterial stiffness and risk of coronary heart disease and stroke: The Rotterdam Study. *Circulation*, 113(5), pp.657–663.

Mcveigh GE, Bank AJ, Cohn JN. Arterial Compliance. In: *Cardiovascular Medicine*.; 2007. pp. 1811-1831.

Meijer WT, Hoes AW, Rutgers D, Bots ML, Hofman A, Grobbee DE. Peripheral arterial disease in the elderly: The Rotterdam Study. *Arterioscler Thromb Vasc Biol*. 1998;18(2):185-192. doi:10.1161/01.ATV.18.2.185.

Mendis, S., Puska, P. & Norrving, B., 2011. Global atlas on cardiovascular disease prevention and control. *World Health Organization*, pp.2–14.

Mitchell, G.F. et al., 2004. Changes in arterial stiffness and wave reflection with advancing age in healthy men and women: The Framingham Heart Study. *Hypertension*, 43(6), pp.1239–1245.

Naghavi, M. et al., 2006. From Vulnerable Plaque to Vulnerable Patient-Part III: Executive Summary of the Screening for Heart Attack Prevention and Education (SHAPE) Task Force Report. *American Journal of Cardiology*, 98(2 SUPPL. 1), pp.2–15.

Nam, S.C. et al., 2010. Factors affecting the validity of ankle-brachial index in the diagnosis of peripheral arterial obstructive disease. *Angiology*, 61(4), pp.392–396.

Norgren, L. et al., 2007. Inter-Society Consensus for the management of peripheral arterial disease (TASC II). *International Angiology*, 26(2), pp.82–157.

Nwankwo, T. et al., 2013. Hypertension among adults in the United States: National Health and Nutrition Examination Survey, 2011-2012. *NCHS data brief*, (133), pp.1–8. Available at: http://www.ncbi.nlm.nih.gov/pubmed/24171916.

O'Rourke, M.F. et al., 2002. Clinical applications of arterial stiffness; definitions and reference values. *American Journal of Hypertension*, 15(5), pp.426–444.

O'Rourke, M.F. & Yaginuma, T., 1984. Wave reflections and the arterial pulse. *Archives of internal medicine*, 144(2), pp.366–371.

Olufsen, M.S. et al., 2000. Numerical simulation and experimental validation of blood flow in arteries with structured-tree outflow conditions. *Annals of Biomedical Engineering*, 28(11), pp.1281–1299.

Olufsen, M.S., 1999. Structured tree outflow condition for blood flow in larger systemic arteries. *The American journal of physiology*, 276(1 Pt 2), pp.H257–H268.

Orchard, T.J. & Strandness, D.E., 1993. Assessment of peripheral vascular disease in diabetes: report and recommendation of an international workshop. *Diabetes Care*, 83(12), pp.685–695.

Pannier, B.M. et al., 2002. Methods and devices for measuring arterial compliance in humans. *American Journal of Hypertension*, 15(8), pp.743–753.

Pasterkamp, G. et al., 1995. Paradoxical arterial wall shrinkage may contribute to luminal narrowing of human atherosclerotic femoral arteries. *Circulation*, 91(5), pp.1444–1449.

Quarteroni A, Veneziani A. Analysis Of A Geometrical Multiscale Model Based on The Coupling of ODEs and PDEs for Blood Flow. 2003;1(2):173-195.

Rashedi, M. et al., 2013. Comparative Study on Tube-Load Modeling of Arterial Hemodynamics in Humans. *ASME Journal of Biomechanics*, 135(March), p.31005.

Sagawa, K., Lie, R.K. & Schaefer, J., 1990. Translation of Otto Frank's Paper "Die Grundform des Arteriellen Pulses" Zeitschrift fur Biologie 37: 483-526 (1899). *Journal of Molecular and Cellular Cardiology*, 22(3), pp.253–277.

Search, H. et al., In vivo arterial compliance in man. , 201.

Shapiro, A.H., 1974. A Computer Simulation of Arterial Dynamics in the Human Leg. *J. Biomachanics*.

Sherwin, S.J. et al., 2003. Computational modelling of 1D blood flow with variable mechanical properties and its application to the simulation of wave propagation in the human arterial system. *International Journal for Numerical Methods In Fluids*, 43(6-7), pp.673–700.

Shim, Y. et al., 1994. Arterial windkessel parameter estimation: A new time-domain method. *Annals of Biomedical Engineering*, 22(1), pp.66–77.

Solà, J. et al., 2011. Chest pulse-wave velocity: A novel approach to assess arterial stiffness. *IEEE Transactions on Biomedical Engineering*, 58(1), pp.215–223.

Stergiopulos, N., Meister, J.J. & Westerhof, N., 1995. Evaluation of methods for estimation of total arterial compliance. *The American journal of physiology*, 268(4 Pt 2), pp.H1540–H1548.

Stergiopulos, N., Westerhof, B.E. & Westerhof, N., 1999. Total arterial inertance as the fourth element of the windkessel model. *The American journal of physiology*, 276(1 Pt 2), pp.H81–H88.

Stergiopulos, N., Young, D.F. & Rogge, T.R., 1992. Computer simulation of arterial flow with applications to arterial and aortic stenoses. *Journal of Biomechanics*, 25(12), pp.1477–1488.

Stout, M. & Aims, S., Integration of Flow Mediated Dilatation Into Clinical Practise .

Sun, Z., 2014. Aging, Arterial Stiffness, and Hypertension. *Hypertension*, 65(2), pp.252–256. Available at: http://hyper.ahajournals.org/cgi/doi/10.1161/HYPERTENSIONAHA.114.03617.

Swamy, G., Olivier, N.B. & Mukkamala, R., 2010. Calculation of forward and backward arterial waves by analysis of two pressure waveforms. *IEEE Transactions on Biomedical Engineering*, 57(12), pp.2833–2839.

Taylor, C. a & Figueroa, C. a, 2009. Patient-specific modeling of cardiovascular mechanics. *Annual review of biomedical engineering*, 11, pp.109–134.

Teng, X.F. & Zhang, Y.T., 2006. An evaluation of a PTT-based method for noninvasive and cuffless estimation of arterial blood pressure. *Annual International Conference of the IEEE Engineering in Medicine and Biology - Proceedings*, pp.6049–6052.

Vardoulis, O., Papaioannou, T.G. & Stergiopulos, N., 2012. On the Estimation of Total Arterial Compliance from Aortic Pulse Wave Velocity. *Annals of Biomedical Engineering*, 40(12), pp.1–8.

Van de Vosse, F.N. & Stergiopulos, N., 2011. Pulse Wave Propagation in the Arterial Tree. *Annual Review of Fluid Mechanics*, 43(1), pp.467–499.

Weintraub, W.S. et al., 2011. Value of primordial and primary prevention for cardiovascular disease: A policy statement from the American Heart Association. *Circulation*, 124(8), pp.967–990.

Westerhof, N. et al., 1972. Forward and backward waves in the arterial system. *Cardiovascular Research*, 6(6), pp.648–656.

Westerhof, N., Elzinga, G. & Sipkema, P., 1971. An artificial arterial system for pumping hearts. *Journal of applied physiology (Bethesda, Md. : 1985)*, 31(5), pp.776–781.

Westerhof, N., Lankhaar, J.W. & Westerhof, B.E., 2009. The arterial windkessel. *Medical and Biological Engineering and Computing*, 47(2), pp.131–141.

White, F.M., 2009. Fluid Mechanics. *McGraw-Hill*, p.1024.

Willens, H.J. et al., 2003. Relationship of Peripheral Arterial Compliance and Standard Cardiovascular Risk Factors. *Vascular and Endovascular Surgery*, 37(3), pp.197–206.

Womersley, J.R., 1957. Oscillatory flow in arteries: the constrained elastic tube as a model of arterial flow and pulse transmission. *Physics in medicine and biology*, 2(2), pp.178–187.

Zhang, G., Hahn, J.O. & Mukkamala, R., 2011. Tube-load model parameter estimation for monitoring arterial hemodynamics. *Frontiers in Physiology*, 2 NOV, pp.1–18.

Zhaopeng Fan, Gong Zhang, S.L., Pulse wave analysis. , 51(6), pp.507–522.

Zipes, D.P. & Wellens, H.J.J., 1998. Clinical Cardiology : New Frontiers Sudden Cardiac Death. , pp.2334–2351.

Zipes, D.P. & Wellens, H.J.J., 1998. Sudden Cardiac Death. *Circulation*, 98(21), pp.2334–2351.

Appendix A Tube-Load Model

In order to find the relation between the pressure waveforms at the two ends of the tube-load model, the analogy between the tube-load model and the transmission line in the microwave circuit were used as defined in the references [1]–[3].

For the tube-load model shown in the Figure A-1, the pressure and flow waveforms can be written as:

$$P(x,t) = P_f(x,t) + P_b(x,t) \quad \text{(A-1)}$$

$$Q(x,t) = Q_f(x,t) - Q_b(x,t) \quad \text{(A-2)}$$

In this equation, P_t and Q_t indicate transferred pressure and flow waveform respectively. Whereas the P_f and Q_f show forward waveforms and the P_b and Q_b stand for backward waveforms as shown in the Figure A-2.

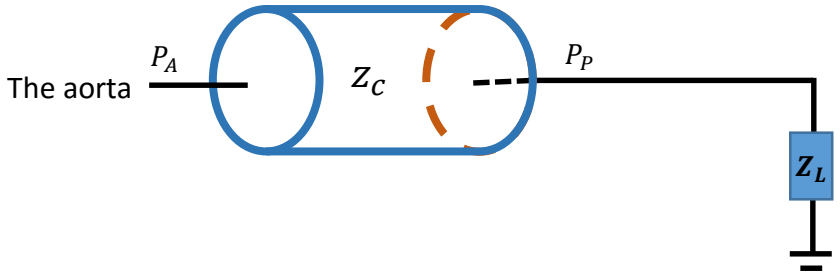

Figure A- 1- Tube-load model of the arterial tree.

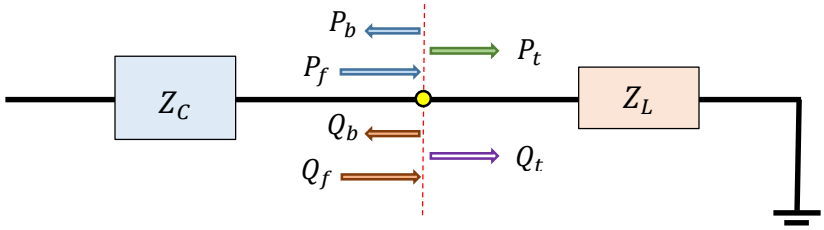

Figure A- 2- The reflection site at the tube load model and forward, backward and transferred waveforms of the pressure and flow.

Using the analogy of the transmission line in microwave theory and the wave propagation in the arterial tree, by applying the conservation of the flow at the reflection site, as it applies for the equivalent electric circuit, the relation between flow and pressure can be described using Z_L[1] as follows:

$$Z_L = \frac{P_t(t)}{Q_t(t)} = \frac{P_f(0,t) + P_b(0,t)}{Q_f(0,t) - Q_b(0,t)} \quad \text{(A-3)}$$

$P_f(0,t)$ and $P_b(0,t)$ show the forward and backward pressure at the reflection site, while $Q_f(0,t)$ and $Q_b(0,t)$ similarly indicate the forward and backward flow at the reflection site. While by using the same analogy, the characteristic impedance is defined as follows:

$$Z_c = \frac{P_f(0,t)}{Q_f(0,t)} = -\frac{P_b(0,t)}{Q_b(0,t)} \quad \text{(A-4)}$$

by applying the same analogy, the coefficient of reflection is defined as follows:

$$\Gamma = \frac{P_b(0,t)}{P_f(0,t)} \quad \text{(A-5)}$$

Replacing the equation (A-4) and (A-5) into the equation (A-3), the following equation will be found:

$$Z_L = \frac{P_t(t)}{Q_t(t)} = \frac{P_f(0,t) + P_b(0,t)}{Z_c(P_f(0,t) - P_b(0,t))} = \frac{P_f(0,t)(1+\Gamma)}{Z_c(P_f(0,t)(1-\Gamma))} = \frac{(1+\Gamma)}{Z_c(1-\Gamma)} \quad \text{(A-6)}$$

Solving this equation for the value of reflection coefficient, Γ results in the following equation:

$$\Gamma = \frac{Z_L - Z_C}{Z_L + Z_C} \quad \text{(A-7)}$$

Moreover, the forward or backward pressure at each point of the arteries can be approximated using the pressure at reflection site by considering the delay. The relation in the frequency domain can be written as in equation (A-8) and (A-9). In this equation, $x = 0$ indicates the reflection site.

$$P_f(x,t) = P_f(x=0,t).e^{-j\omega\tau\frac{x}{d}} \quad \text{(A-8)}$$

$$P_b(x,t) = P_b(x=0,t).e^{j\omega\tau\frac{x}{d}} \quad \text{(A-9)}$$

In this equation, τ stands for pulse transit time (PTT) and "d" shows the length of the tube which in this case is the distance between the aortic valve and the peripheries. PTT is defined as the time

that takes to take the pulse wave to get from one end of the tube to the other end. Substituting the equations (A-8) and (A-9) into equation (4-1), results in the following formulation:

$$P(x,t) = P_f(x_{=0},t).e^{-j\omega\tau\frac{x}{d}} + P_b(x_{=0},t).e^{j\omega\tau\frac{x}{d}} \quad \text{(A-10)}$$

Based on this equation, the pressure close to the aortic valve, where the x equals the value "d", can be explained as in the equation (A-11). Similarly, for the reflection site where x equals the value of zero, the blood pressure can be expressed in the equation (A-12).

$$P_{Aorta} = P(d,t) = P_f(0,t).e^{-j\omega\tau} + P_b(0,t).e^{j\omega\tau} \quad \text{(A-11)}$$

$$P_P = P(0,t) = P_f(0,t) + P_b(0,t) \quad \text{(A-12)}$$

Using the reflection coefficient, the equations (A-11) and (A-12) can be written as follows.

$$P_{Aorta} = P_f(0,t)[e^{-j\omega\tau} + \Gamma.e^{j\omega\tau}] \quad \text{(A-13)}$$

$$P_P = P_f(0,t)[1+\Gamma] \quad \text{(A-14)}$$

Therefore, the relation between the pressure waveforms at the aorta and the peripheries can be written as follow:

$$\frac{P_{Aorta}}{P_P} = \frac{e^{-j\omega\tau} + \Gamma.e^{j\omega\tau}}{1+\Gamma} \quad \text{(A-15)}$$

References:

[1] D. Pozar, Microwave Engineering. , John Wiley & Sons, 2005.

[2] M. Rashedi, N. Fazeli, a Chappell, S. Wang, R. MacArthur, M. S. McMurtry, B. a Finegan, and J. O. Hahn, "Comparative Study on Tube-Load Modeling of Arterial Hemodynamics in Humans," *ASME J. Biomech.*, vol. 135, no. March, p. 31005, 2013.

[3] G. Zhang, J. O. Hahn, and R. Mukkamala, "Tube-load model parameter estimation for monitoring arterial hemodynamics," *Front. Physiol.*, vol. 2,cno. November, pp. 1–18, 2011.

Appendix B The Arterial Tree Simulator

In this section more information regarding the model of the arterial tree introduced by M. Olufsen is provided. All of the material in this section is provided from references [1], [2]. In this thesis, the model was used for simulating CVD cases. It should be noted that the code was provided by Dr. Olufsen.

B.1 - Geometrical Information

In this model the entire arterial tree is divided into 29 smaller sections connected together as shown in the figure B-1. The length and the radius of each section is set as they were measured for a specific subject. The measurement was done directly using the MRI images.

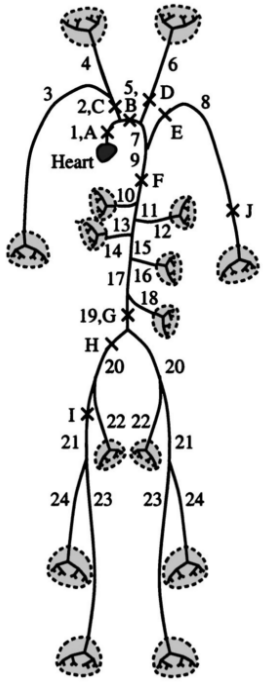

Figure B- 1 - Modeling the arterial tree in the reference [2]

The model accounts for the tapering along the arteries and formulates the radius at each point of the artery by the following equation:

$$r_o(x) = r_t \exp\left(\log(\frac{r_b}{r_t})\frac{x}{L}\right) \quad \text{(B-1)}$$

with r_t and r_b showing the inlet and outlet radius respectively as shown in the Figure B-2. Where

x stands for the distance between the top side of the artery while L shows the total length of the artery. The value of these parameter for each artery is shown in the table B-1.

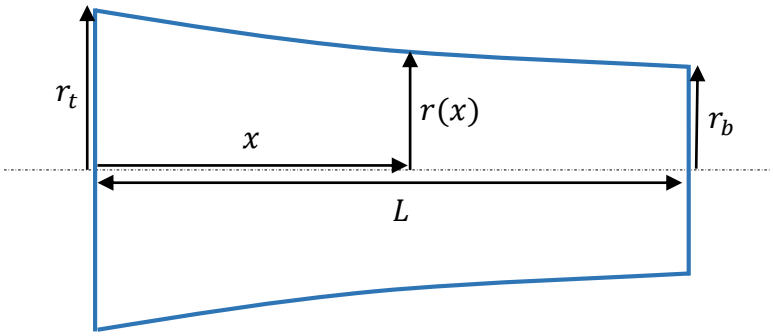

Figure B-2 – Tapering along the length of an artery (adapted from [2]).

Table B - 1 - geometrical data of the arterial tree used in [2]

Number	*Artery*	*Length(cm)*	$r_t(cm)$	$r_b(cm)$
1	*Ascending Aorta*	7.0	1.25	1.14
2	*Anonyma*	3.5	0.7	0.7
3	*Right Subclavian*	43.0	0.44	0.28
4	*Right Carotid*	17.0	0.29	0.28
5	*Aortic Arch*	1.8	1.14	1.11
6	*Left Carotid*	19.0	0.29	0.28
7	*Aortic Arch*	1.0	1.11	1.09
8	*Left Subclavian*	43.0	0.44	0.28
9	*Thoracic Aorta*	18.8	1.09	0.85
10	*Celiac Axis*	3.0	0.33	0.30
11	*Abdominal Aorta*	2.0	0.85	0.83
12	*Superior Mesentric*	5.0	0.33	0.33
13	*Abdominal Aorta*	2.0	0.83	0.80
14	*Renal*	3.0	0.28	0.25
15	*Abdominal Aorta*	1.0	0.80	0.79
16	*Renal*	3.0	0.28	0.25
17	*Abdominal Aorta*	6.0	0.79	0.73
18	*Inferior Mesentric*	4.0	0.20	0.18
19	*Abdominal Aorta*	3.0	0.73	0.70
20	*External Illiac*	6.5	0.45	0.43
21	*Femoral*	13.0	0.43	0.40
22	*Internal Illiac*	4.5	0.20	0.20
23	*Deep Femoral*	11.0	0.20	0.20
24	*Femoral*	44.0	0.40	0.30

B.2 - Adding Tibial Arteries Into the Original Arterial Model

In order to be able to evaluate the value of ABI for the PAD simulations, posterior and inferior tibial arteries were added to the original arterial model, introduced in the [2]. Since there was no access to geometrical information of the participant of the original paper, the values for the length and the radius of the subject were estimated based on the literature and by considering the following criteria:

1. ***The length of the tibial should be close to 1 foot, while the inlet radius should be smaller than the outlet radius of the femoral, yet bigger than the half of its value (based on the branching rule in the arterial tree).*** Different values for the length and the radius of the radius were suggested and check for meeting other criteria.

2. ***The effect of adding tibials should be minimal on the femoral, brachial and the aortic flow and pressure waveforms.*** In order to evaluate the magnitude of the effect of the addition of tibilais, the RMSE of the original and secondary value of these waveforms were calculated. The mean value of these waveform were also compared to the value of the original value.
3. ***ABI close to 1.*** One of the other criterial for the tibial of the subject, which was known to be healthy was to have a ABI (ratio of the systolic pressure at the ankle to the brachial to be close to 1).

8 cases of many simulations of tibial are listed in the table B-2. Finally, based on the criteria defined above, tibial 8 was chosen. All of the simulation was one done on the arterial tree with added tibials.

Table B - 2 - Different trials for the tibial artery

Number	*Length(cm)*	$r_{top}(cm)$	$r_{end}(cm)$	$\overline{P_3}$	$\overline{P_i}$	$\overline{Q_3}$	$\overline{Q_{24}}$	ABI
1	*32.0*	0.22	0.16	100.31	102.19	1.90	3.09	0.9
2	*32.0*	0.20	0.20	99.20	98.86	1.85	4.48	0.8
3	*32.0*	0.22	0.14	101.18	104.88	1.93	1.96	1.0
4	*32.0*	0.22	0.10	102.08	107.34	1.97	0.85	0.9
5	*32.0*	0.20	0.18	102.13	107.42	1.97	0.81	0.9
6	*32.0*	0.22	0.14	101.18	104.88	1.93	1.96	0.9
7	*32.0*	0.25	0.14	101.07	104.63	1.93	2.07	1.0
8	*28.0*	0.26	0.14	100.31	102.19	1.90	3.09	1.0

B.3 - Adding Blockage into Femoral Artery

According to the equation (B-2), once the values of r_b, $r_t$and L are set, the radius at each point will automatically be calculated. Therefore, in this model local narrowing such as in the PAD cannot be applied to the arteries. One of the solutions to address this problem, was to divide the femoral (artery 24 in the figure B-1) into three section in a way that the total length of the femoral remains the same.

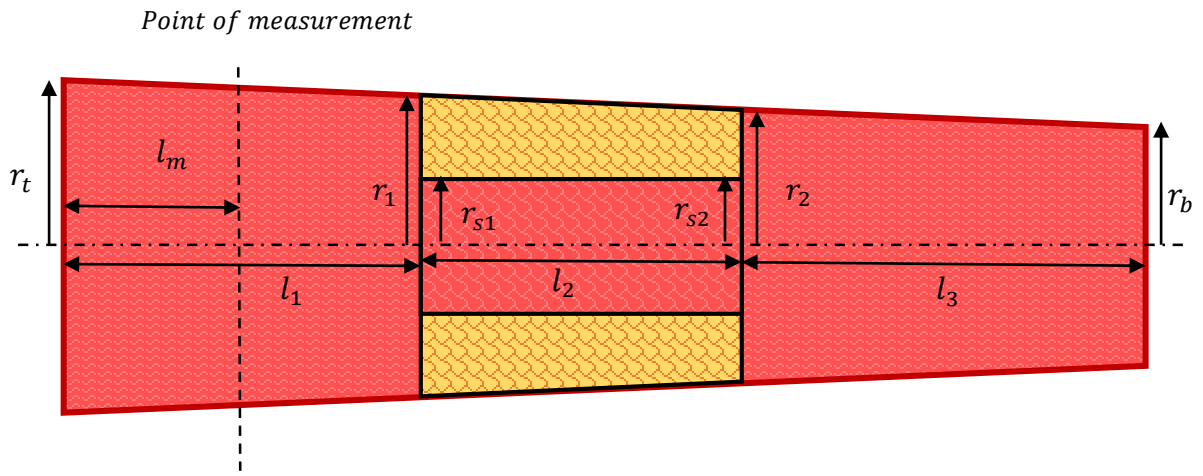

Figure B-3 -Dividing the femoral (artery number 24) into three subsections.

B.4 - Simulations of CVD

In order to have a consistent baseline for all of the simulations, the geometries of the femoral in a healthy arterial tree, were set as the values shown in the table B-2. These values are for a case that no blockages exists.

Table B - 3 - Dividing the femoral artery into three sections.

Parameters	l_1	l_2	l_3	r_t	r_b	r_1=r_{s1}	r_2=r_{s2}
Value(cm)	15.0	2.0	27.0	0.4	0.3	0.36	0.36

B.5 - Simulations of PAD in the Femoral Artery

In this thesis, different scenarios of femoral PAD were simulated in the arterial tree model. The detailed information of these simulation is listed in the Table B-4. Each variable is measured as shown in the Figure B-3.

Table B - 4 - Simulating the PAD blockage into the femoral artery.

Simulaion #	$l_1(cm)$	$l_2(cm)$	$l_3(cm)$	$r_1(cm)$	$r_2(cm)$	$r_{s1} = r_{s2}$	A%
FS_1	15.0	2	27	0.36	0.36	0.3	32.71
FS_2	15.0	4	25	0.36	0.35	0.3	32.71
FS_3	15.0	6	23	0.36	0.35	0.3	32.71
FS_4	15.0	8	21	0.36	0.34	0.3	32.71
FS_5	15.0	10	19	0.36	0.34	0.3	32.71
FS_6	15.0	2	27	0.36	0.36	0.25	53.27
FS_7	15.0	4	25	0.36	0.35	0.25	53.27
FS_8	15.0	6	23	0.36	0.35	0.25	53.27
FS_9	15.0	8	21	0.36	0.34	0.25	53.27
FS_10	15.0	10	19	0.36	0.34	0.25	53.27
FS_11	15.0	2	27	0.36	0.36	0.2	70.10
FS_12	15.0	4	25	0.36	0.35	0.2	70.10
FS_13	15.0	6	23	0.36	0.35	0.2	70.10
FS_14	15.0	8	21	0.36	0.34	0.2	70.10
FS_15	15.0	10	19	0.36	0.34	0.2	70.10
FS_16	15.0	2	27	0.36	0.36	0.15	83.18
FS_17	15.0	4	25	0.36	0.35	0.15	83.18
FS_18	15.0	6	23	0.36	0.35	0.15	83.18
FS_19	15.0	8	21	0.36	0.34	0.15	83.18
FS_20	15.0	10	19	0.36	0.34	0.15	83.18

B.6 - Result of the simulations of PAD

The result of the parameter estimation, including the RMSE error and the parameters of the tube-load model for these set of the simulation is presented in the Table B-4. As this table shows, for these simulations that cover mild to severe obstruction the PTT is constant with 5% tolerance (Figure B-4(a)). Parameter α decreases as much as 100% (Figure B-4(b)), while β decrease with 50% change (Figure B-4(c)).

Table B - 5 - Determining the tube-load model parameters for simulation of PAD blockages in the femoral artery.

Simulaion #	$Length\ of\ blockage(cm)$	$r_{s1} = r_{s2}$	A%	PTT	α	β	RMSE
Normal	-	-	0	0.169	15.913	0.845	1.011
FS_1	2	0.3	32.71	0.169	13.033	0.843	0.954
FS_2	4	0.3	32.71	0.169	10.760	0.838	0.907
FS_3	6	0.3	32.71	0.169	9.103	0.833	0.876
FS_4	8	0.3	32.71	0.170	6.889	0.825	0.854
FS_5	10	0.3	32.71	0.170	5.924	0.820	0.842
FS_6	2	0.25	53.27	0.169	8.630	0.838	0.864
FS_7	4	0.25	53.27	0.170	2.873	0.820	0.845
FS_8	6	0.25	53.27	0.170	0.010	0.801	0.924
FS_9	8	0.25	53.27	0.169	0.010	0.781	1.066
FS_10	10	0.25	53.27	0.168	0.010	0.763	1.212
FS_11	2	0.2	70.10	0.170	0.010	0.806	0.894
FS_12	4	0.2	70.10	0.166	0.010	0.751	1.436
FS_13	6	0.2	70.10	0.163	0.010	0.700	1.840
FS_14	8	0.2	70.10	0.162	0.010	0.660	2.100
FS_15	10	0.2	70.10	0.161	0.010	0.629	2.270
FS_16	2	0.15	83.18	0.162	0.010	0.663	2.092
FS_17	4	0.15	83.18	0.160	0.010	0.570	2.584
FS_18	6	0.15	83.18	0.160	0.010	0.528	2.788
FS_19	8	0.15	83.18	0.160	0.010	0.505	2.902
FS_20	10	0.15	83.18	0.160	0.010	0.491	2.975

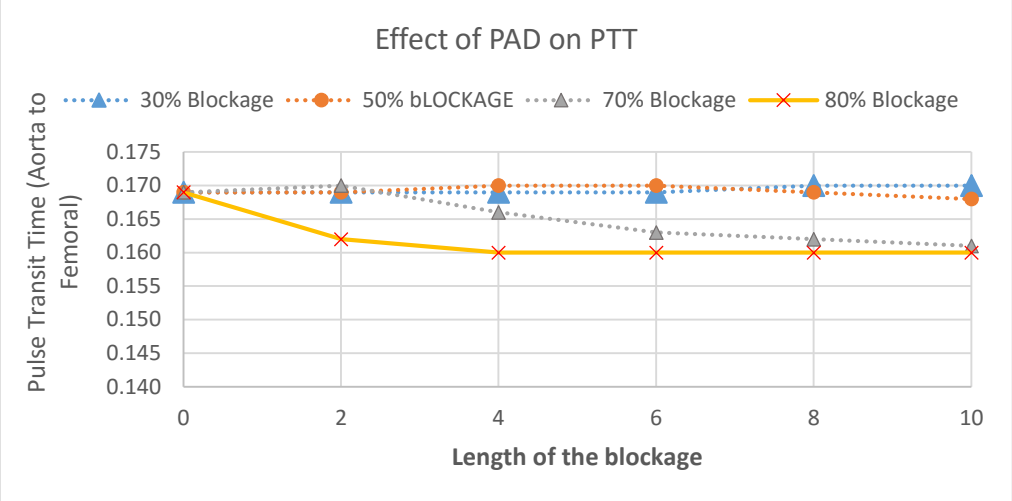

(a)

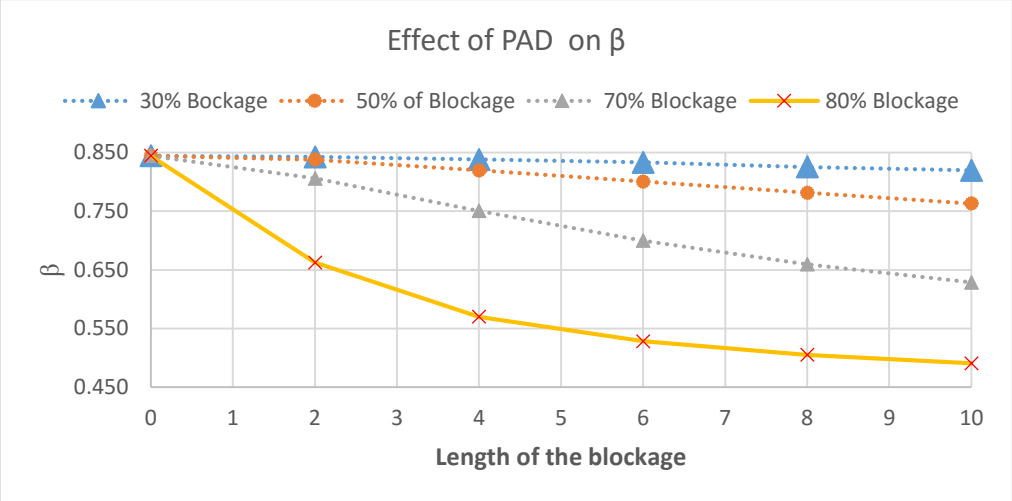

(b)

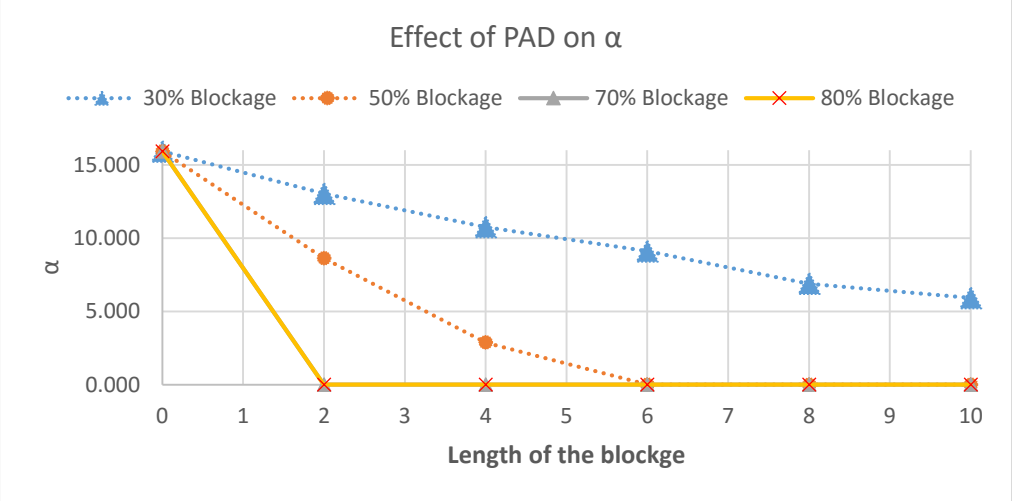

(c)

Figure B-4 – Effect of femoral stenosis on the parameters of the tube-load model.

References:

[1] M. S. Olufsen, “Structured tree outflow condition for blood flow in larger systemic arteries.,” *Am. J. Physiol.*, vol. 276, no. 1 Pt 2, pp. H257–H268, 1999.

[2] M. S. Olufsen, C. S. Peskin, W. Y. Kim, E. M. Pedersen, A. Nadim, and J. Larsen, “Numerical simulation and experimental validation of blood flow in arteries with structured-tree outflow conditions,” *Ann. Biomed. Eng.*, vol. 28, no. 11, pp. 1281–1299, 2000.